AD-A027 706

USADAC TECHNICAL LIBRARY
5 0712 01021373 3

FORTIFIKATORISK

NOTAT NR. 80 / 72

UNDERGROUND AMMUNITION STORAGE

Report I

Test Programme, Instrumentation, and Data Reduction

BEST AVAILABLE COPY

SEP 1975

DISTRIBUTION STATEMENT A
Approved for public release;
Distribution Unlimited

FORSVARETS BYGNINGSTJENESTE

NORWEGIAN DEFENCE CONSTRUCTION SERVICE
Office of Test and Development

Fortifikatorisk notat nr 80/72

UNDERGROUND AMMUNITION STORAGE

Report I

Test Programme, Instrumentation, and Data Reduction

by

A. Skjeltorp, T. Hegdahl, and A. Jenssen

September 1975

DISTRIBUTION STATEMENT A
Approved for public release;
Distribution Unlimited

TABLE OF CONTENTS

ABSTRACT

This report is the first in a series of five describing an extensive series of model tests on air blast propagation in underground ammunition storage sites. A general description is given of the scope and purpose of the tests as well as a presentation of the principles of scaling and various intrinsic uncertainties which may cause problems in the modelling technique. The report also surveys the test programme, instrumentation, and data reduction for the whole test series.

1. INTRODUCTION

This report is the first in a series of five /1-6/* describing an extenive series of model tests on air blast propagation in underground ammunition storage sites.

These tests are a natural continuation of earlier work performed by this office in this general field /7-12/.

1.1 Study Objectives

The basic objectives for performing these tests have been to use several empirical and theoretical scaling techniques to combine air blast data into a form that allows the prediction of blast wave propagation inside a wide range of typical underground ammunition storage sites as a function of explosive quantities and geometrical parameters. These methods of predictions will thus give the design engineer a tool to evaluate the effects of different layouts and geometries. In particular, it will be possible to specify the necessary strength of blast doors, blast valves and blast walls to prevent the propagation of detonation from one chamber to another in a connected chamber storage site. Furthermore, in the determination of the pressure and impulse at the exit of the tunnel leading into the underground storage complex, it will be possible to determine the hazardous area around such a site /13, 14/.

1.2 Problem Background

The detailed analysis of accidental explosions in underground ammunition storage sites in regard to blast wave propagation generally involves three distinct steps:

Determination of the pressure-time history in the storage chamber; determination of the blast wave propagation from the storage chamber down the main passageway (or between chambers in connected chamber

* Numerals in / / designate appended references

storage sites); and finally, mapping of the blast wave emerging from the exit of the tunnel in the terrain outside. This analysis can generally be performed in three ways: full scale testing; theoretical calculations; or finally, model testing.

As far as theoretical treatment is concerned, one can in principle describe the blast propagation by sets of mathematical equations, and attempt to solve these equations numerically. However, the methods of computation are often so involved that one cannot economically repeat these computations while varying in a systematic manner all of the physical parameters which may affect the blast wave. One important point to remember is that one has no idea of the accuracy of such theoretical solutions until proof tested.

The second possibility is experimental studies in large or full scale. Such tests would, however, be very costly, take long time and also cause instrumentation and manning problems. This would limit the number of tests to a very few special cases, and there could be a tendency to draw conclusions outside the range of the actual experimental and geometrical conditions.

The third and last possibility is model testing using similarity methods. This method forms the basis for the experiments presented in the present reports.

1.3 Scope of Report

The general principles of scaling are presented in Sec.2 together with a discussion of various intrinsic uncertainties which may cause problems in the modelling technique. The test plan and models are described in Sec.3 followed by a presentation of the instrumentation in Sec.4. Section 5 contains a description of the data reduction and a discussion of the experimental errors.

The appendices provide more detailed sources of information of the data reduction and analysis for this whole series of reports.

Because several terms that relate to blast propagation in underground ammunition storage are used differently by different authors, a list of definitions is also included as a separate appendix.

2. THEORETICAL CONSIDERATIONS

2.1 Scaling Relationships

The basis for the scaling relationships used in the present work correspond to the familiar Hopkinson scaling laws /15/. The use of models requires complete geometrical similarity between the model and the full scale system. If the linear scale factor is n, the relationship between distances in the full scale (subcript F) and model (subscript M) is

$$L_F = nL_M \qquad (2.1\ a)$$

Likewise, areas scale as

$$A_F = n^2 A_M, \qquad (2.1\ b)$$

and volumes as

$$V_F = n^3 V_M \qquad (2.1\ c)$$

For the energy release

$$E_F = n^3 E_M \qquad (2.1\ d)$$

This energy scaling is also valid for the explosive quantity if the energy release per unit weight is constant:

$$Q_F = n^3 Q_M \qquad (2.1\ e)$$

The blast wave parameters scale as

$$p_F = p_M \qquad (2.1\ f)$$

for peak pressure, and

$$I_F = nI_M \qquad (2.1\ g)$$

for impulse, and

$$t_F = nt_M \qquad (2.1\ h)$$

for characteristic times.

Inherent in this simple scaling is the assumption of perfect gas behaviour of air and no differences in ambient conditions (e.g. temperature and pressure) between the model and prototype. Furthermore, the theory does not account for energy dissipating effects due to tunnel or chamber walls such as: thermal energy transmission to the walls; elastic or inelastic deformation of the walls; viscous loss due to wall roughness.

If one tried to scale all these effects properly from a full scale system, it would require tests in scale 1:1. It is therefore important to try to put an upper limit on the uncertainties involved in neglecting non-scaled effects. This will be attempted in Sec.2.2 - 2.4, and it will be shown that the effects from these sources will be relatively unimportant except maybe for the viscous loss due to wall roughness. However, as the relative wall roughness is normally significantly larger in a full scale site than in a steel model, the model data would tend to be conservative or on the safe side.

As will be discussed in the succeeding reports, careful inspection of the experimental results from the various model tests have produced extended <u>empirical scaling relationships</u> representing a wide range of important geometrical parameters. One should note

the distinction between scaling laws and scaling relationships in this connection as the former require complete geometrical similarity between the model and the prototype.

2.2 Effects of Thermal Interactions with the Walls

The detonation of explosives in confined regions such as storage chambers produces hot gases from which energy is transferred by heat flow to the much cooler confining walls. There are two mechanisms involved in this heat transfer: Radiation and a combination of conduction and convection. In that the surrounding medium is rock in the full scale case and steel in the present model tests, the heat losses do not scale due to the large difference in thermal properties.

The question is therefore whether these effects will be of such magnitude that it will introduce large systematic errors in the scaled data.

Earlier theoretical calculations have been carried out to estimate the heat conduction in a detonation chamber in full scale (rock) and steel models in linear scales 1:10 and 1:100 /16/. The basic results are reproduced in Fig.2.2 for a loading density of 100 kg TNT/m^3. It can be seen that for the full scale case (chamber radius R_o = 6 m), the heat loss is relatively unimportant. For a steel model in a linear scale 1:100, the heat loss is estimated to be about 14% of the total heat at a scaled time t/R_c = 20 ms/m, corresponding to 120 ms in the full scale case /17/. Qualitative arguments have also been given to the effect that the relative heat loss increases with decreasing loading densities and that the result from a 1:100 steel model at low loading densities are expected to be quite misleading unless a heat loss correction is applied. Fortunately, the present series of experiments offers some results which can be used to check these conclusions. However, first an attempt will be made to convert the thermal loss into pressure effects. This cannot be

performed in a straightforward way, but to first order the pressure decrease in an unvented chamber due to conduction loss can be roughly described as /18/

$$\frac{dp}{dt} = \frac{dE_c}{dt}(\gamma - 1)/V \qquad (2.2\ a)$$

Here, dE_c/dt is the heat loss in watts, V is the chamber volume, and $\gamma = c_p/c_v$ the usual specific heat ratio for the detonation products. Assuming γ to be constant, the relative pressure decrease can be found from Eq. (2.2 a) to be approximately equal to the relative heat loss

$$\frac{dp}{p} \simeq \frac{dE_c}{E_t} \qquad (2.2\ b)$$

Another heat transfer which produces pressure decay, is radiation. There are indications that conduction effects at the high temperatures of internal explosions are less than those of radiation /18/. However, the radiation loss is expected to produce approximately the same effects whether the confining walls are rock or steel.

Relatively good experimental estimates of the maximum effects on peak pressure and positive impulse of the heat loss are provided by the closed bomb tests in Report II A /1/, and the connected chamber storage tests in Report IV A /2/. Details are given in these reports and only one example will be discussed here. In one typical closed bomb test with a loading density of 11 kg TNT/m3 (effective chamber radius $R_o \simeq$ 0,15 m), it was found that the pressure fell approximately 15% in the first t/R_o = 20 ms/m scaled time. In the following t/R_o = 200 ms/m the pressure fell only about 5%.

These pressure drops are considered to be upper limits for the effects from heat loss due to conduction in as much as part of the pressure drops found in these tests are in fact due to small leaks in the detonation chamber (Sec. 3.5)as well as radiation loss. As noted earlier, the effects from radiation probably exceed those of conduction. From this particular test and from similar observations of the other test results referred to earlier, it is therefore concluded that the heat loss will be of no practical importance as to the correctness of scaling the present steel model results to full scale installations in rock. Thus, the calculations in Ref. 16 appear to overestimate the effects from heat loss in this connection.

One possible explanation is that the steel walls are assumed to be completely clean. This is far from being true under normal experimental conditions. The walls will be somewhat corroded and covered with soot due to the incomplete detonation of TNT. This will certainly reduce the effective heat transfer to the steel, but it is hardly possible to be more spesific on this point without detailed calculations.

2.3 Mechanical Interactions with the Walls

It is of interest to put some upper limits on the effects from elastic or plastic deformations of the chamber walls in the present tests. Steel is elastic up to approximately 200 kbar and there will be negligible direct energy loss at the present pressure levels (Report II A). However, due to the oscillations of the pressure-time history (Report II A), the chamber walls will also oscillate. This will cause some changes in the blast wave emerging from the chamber with a small lowering of the pressure and an increase in the duration of the blast wave.

For the simplified case of a spherical chamber shown in Fig. 2.3, it can be shown that the deformation energy from a step load is approximately given by

$$E_D = 2\pi \frac{R_1^3}{R_2^3 - R_1^3} \left(\frac{R_1^3}{2\mu_L + 3\lambda_L} + \frac{R_2^3}{4\mu_L} \right) p^2 \qquad (2.3)$$

with parameters defined in Fig. 2.3.

To evaluate E_D relative to the total energy release, one particular case will be considered with the following values /19/:

Q = 51,5 g TNT

V_1 = 300 cm^3 = volume of detonation chamber

V_2 = 24500 cm^3 = total volume of chamber

This produces

$Q/V_1 \simeq$ 172 kg/m3 = loading density

with an average chamber pressure of (Report II A)

$p \simeq$ 2000 bar

The total energy release is

$E_t \sim 1{,}4 \times 10^5$ Joule (2700 Joule/g TNT).

The volumes V_1 and V_2 correspond to the following equivalent spherical radii:

R_1 = 4,2 cm

R_2 = 18,0 cm.

Using these values and the values given in Fig. 2.3 for steel, Eq. (2.3) produces the total deformation energy

E_D = 58 Joule

and relative to the total energy release

$$E_D/E_t \sim 4 \times 10^{-4} \quad \text{or } 0{,}04\%.$$

As $p \propto E_t$, this shows that the mechanical interaction with the walls is expected to have a negligible effect on the front pressure.

This can be compared with a corresponding full scale chamber in granite (with the same geometry as in Fig. 2.3) in a linear scale 100:1 of the model. Using the material constants in Fig. 2.3, the relative deformation energy is approximately

$$E_D/E_t \sim 0{,}4\%$$

or ten times as high as for the steel model. (This can be seen immediately as the elastisity module for steel is approximately ten times as high as the elastisity module for granite).

The general conclusion which can be drawn from these approximate calculations is that the energy loss due to elastic deformation of the chamber walls will not significantly affect the scaling relationships between the present model tests and prototype installations in rock.

The preceeding analysis is based on the assumption of elastic deformations of the detonation chamber. In practice, however, there will also be small permanent deformations of the chamber and exit tube (visual inspection after many shots). It is reasonable to assume that this will produce negligible energy losses. This will also be the case for prototype installations in rock with sufficient overhead cover to prevent venting, as the destruction is expected to take place in the vicinity of cracks and flaws in the rock. Even with the destruction of inner concrete liner walls, the relative energy loss is expected to be less than 1% /20/.

In the model tests, shock waves in the air surrounding the model will also be generated. The energy of these must be transmitted through the steel walls, and has to be less than the deformation energy taken up by the model. This type of energy loss can therefore also be neglected.

2.4 Viscous Losses to the Walls

There are numerous experimental results pointing to the effect that blast waves in tubes and tunnels may be damped significantly due to viscous losses stemming from wall roughness /21, 22/. In particular, the results from recent large scale tests in rock tunnels in Sweden /23/ and Norway /24/ have showed a viscous damping of typically 40-80% in the average peak overpressure for travel distances of about 20 tunnel diameters. These unusually large damping effects were due to large wall roughnesses which were typically 5-10% of the tunnel diameter.

For the steel models in the present experiments, the viscous damping will be much less as the tube walls are relatively smooth (Sec. 3). This has been clearly demonstrated in earlier tests of one-dimensional blast wave propagation in tubes and tunnels with diameters ranging from 5 to 600 cm /21/. Considering the practical accuracies aimed at in these types of experiments, it was found that the viscous damping could be described adequately using a model originally proposed by Porzel /25, 22/. This model has also been relatively successful in describing the viscous damping in the Swedish tests referred to earlier /26/. It is therefore of interest to outline the results of this model.

From thermodynamics it can be shown that pressure reduction due to wall roughness is given to a good approximation by /25/:

$$Y(p) = \text{constant} - 2\epsilon \frac{\bar{e}}{D} \cdot \frac{L}{D} \qquad (2.4\ a)$$

Here, $Y(p)$ is an impedance function

$$Y(p) = \frac{2\mu + 1}{\mu + 1} \ln p - \frac{\mu}{\mu + 1} \ln (p + \mu + 1) - \frac{1}{p} \qquad (2.4\ b)$$

where p is the dimensionless overpressure ratio $p = p_{so}/p_o$ and p_o = ambient pressure /27/. Furthermore, μ is a thermodynamic parameter

$$\mu = (\gamma + 1)/(\gamma - 1) \qquad (2.4\ c)$$

where γ is the usual ratio of the specific heats, $\gamma = c_p/c_v$. The constant ϵ in Eq. (2.4 a) is a proportionality factor or efficiency with

$$1/2 \leq \epsilon \leq 1 \qquad (2.4\ d)$$

It has been argued that $\epsilon \simeq 1$ for "strong impedance", i.e. in early shock wave formation and $\epsilon \simeq 1/2$ for "weak impedance" or beyond a so-called choke formation in the tunnel. $\bar{e}$ in Eq.(2.4 a) is the average roughness of the tunnel. For engineering purposes, an adequate value can be found from

$$\bar{e} = \int e\,d\,(\text{Area}) / \int d\,(\text{Area}) \qquad (2.4\ e)$$

where e equals the depth of roughness and the area is integrated over the wall of the tunnel. Finally, D = hydraulic diameter = 4 A/S, with A the cross-sectional area and S the tunnel perimeter.

For high pressures, $p \gg \mu$ (= 6 for air with γ = 1,4), Eq.(2.4 a) reduces to $Y(p) = \ln p$ and therefore $\ln p = \text{constant} - 2\epsilon \frac{\bar{e}}{D} \cdot \frac{L}{D}$, which has the solution

$$p(L) = p(L_o)\exp(-k\,\frac{L - L_o}{D}) \qquad (2.4\ f)$$

with an attenuation constant /28, 29/

$$k = 2\epsilon\,\frac{\bar{e}}{D} \qquad (2.4\ g)$$

It is also interesting to note for low pressures, $p \ll \mu$, $Y \simeq -1/p$, the relative pressure attenuation expressed in Eq.(2.4 a) is minutely small compared to the high pressure attenuation in Eq.(2.4 f).

The value for $\bar{e}$ in Eq.(2.4 a) has been fitted to experimental data referred to earlier /21, 30/ and the results show fair agreement with the values for $\bar{e}$ when measured directly.

2.5 Validity of Model and Large Scale Testing

It is often argued that one has no check of the accuracy of model tests unless a direct model-prototype comparison is conducted. In as much as there are relatively few large scale tests on underground ammunition storage, only a few comparisons for very special cases can be made. It will therefore be considered very important, throughout this series of reports to discuss in some detail those comparisons for which both model and prototype data are available. The term "validity of model testing" is often misused as one receives the impression that model-prototype comparison is always needed because the analysis applies similtude technique. One should rather consider the few model-prototype comparisons as tests of the assumptions, and accept the validity of model tests with similar accuracy for analogous problems.

Another important point to remember is that the model tests described in these reports apply methods of obtaining engineering answers to questions which cannot be found more accurately at an acceptable cost any other way. The very few large scale tests conducted up to the present time are not sufficient by

themselves to form a basis for safety criteria. There are several reasons for this:

- There is a lack of systematic investigations for different geometries
- The majority of the test sites are not geometrically similar to sites in use
- Energy losses due to friction and viscous interaction with the walls are expected to be significantly different for several of the tests due to relatively large differences in wall roughness from site to site. This complicates the quantitative comparisons considerably
- There are severe difficulties connected with the instrumentation due to the destructive power from debris and the need for long transmission lines between the pressure transducers and the recording instruments. The interpretation of many of the test results has therefore been quite uncertain
- Attempts to confirm the test results theoretically have so far been inconclusive as to the possibility of extending the results to widely different geometries and providing reliable information of the uncertainties involved

From these general observations it therefore appears that the sparse data from the large scale results should be used with some caution. This is especially true in attempting to generalize or extend the results to a wide range of different geometries. These tests will, however, be quite important for direct comparisons with geometrically similar model tests. In the event of future costly large scale experiments it is considered essential to have these preceded by model tests as an aid in the planning.

3. TEST PROGRAMME AND MODELS

The test programme was divided into four major parts which are reported in the four remaining reports of this series:

3.1 Report II

Closed bomb tests to determine the average pressure exerted on the chamber walls in underground ammunition storage sites. The parameters which were varied in these tests are shown in Fig. 3.1:

V_i = chamber volume
Q = charge weight and type of explosive
A_j = vented area

3.2 Report III

Determination of the blast wave propagation in the passageway of a single chamber storage site. The parameters which were varied in these tests are shown in Fig. 3.2:

V_i = chamber volume

Q = explosive charge weight (TNT)

A_j = passageway cross section

L = distance along passageway

3.3 Report IV

Determination of the blast wave propagation in the main passageway of a connected chamber storage site. The parameters which were varied in these tests are shown in Fig. 3.3:

V_i = chamber volume

Q = explosive charge weight (TNT)

A_j' = branch passageway cross section

A_k = main passageway cross section

v_m = angle between branch and main passageway

L = distance along main passageway

3.4 Report V

Determination of the blast wave propagation between connected chamber storage sites and the blast load on doors in three sites. The different geometries and the parameters which were varied in the tests are shown in Fig. 3.4.

Q = explosive charge weight

L = distance along main passageway

3.5 Model Construction

The chambers were the most critical parts in the construction of the models in regard to strength as average pressures up to 200 bars were expected with pressure peaks up to 8 times this value. This required a type of steel which would not be too brittle and a quality St 50 was chosen. Example of the design of one particular chamber ($V = 15200\ cm^3$) is shown in Fig. 3.5 a with the standard codes used in Norway.

To vary the chamber volume, various insertions were used and some typical examples are shown in Fig. 3.5 b. As may be seen, the inlays were mounted directly on to one of the endpieces of the chamber.

Examples of the connections between chambers and the tubes are shown in Fig. 3.5 c. This figure also shows the design of some of the straight tubes (main passageway) with the pressure gauge mountings.

All chambers, branch passageways and main passageways were cylindrical, but using the cross section of the main passageway as the scale reference, these steel models are ideally thought to be in a linear scale from 1:50 to 1:100 of typical configuration of Norwegian underground storage sites. The difference in the geometry of the cross sections between model and full scale, is thought to have minor influence upon the test result.

4. INSTRUMENTATION

4.1 Pressure Transducers and Measuring Chain

To measure the pressure-time history in the various models, standard instrumentation techniques were employed. The pressure transducers in the detonation chambers and exit tubes were of the Kistler 603 B, 601 H, and 6201 type with rise times of 100 microseconds and a natural frequency of 400 kHz.

The mounting of the transducer in the detonation chamber, as shown in Fig. 4.1 a, was especially designed to reduce the thermal response of the transducer to the high temperatures of the detonation products. To achieve this, a relatively large cavity in front of the transducer was filled with a mixture of silicone oil and graphite. This arrangement is expected to reduce the rise time of the transducer by a factor of about 30, but this will not be critical for the type of experiment reported here. Similar precautions were taken in mounting the transducers in the tubes as shown in Fig. 4.1 b, where a 2 mm thick Silicon rubber plate served as a heat shield. This protection proved to be sufficient as the temperature rise was significantly smaller in the tubes than in the chamber.

The signals from the pressure transducers were processed as shown in Fig. 4.1 c. The output from the charge amplifiers were recorded in either of two different modes:

- Mode A: The pressure-time histories were photographed directly from oscilloscope displays
- Mode B: The pressure recordings were stored on an analog tape recorder and subsequently played back to a CEC U.V. writer using light sensitive paper.

Mode A gives intrinsically the best resolution of about 5 μ sec, compared to an approximate resolution of 25 μ sec for mode B (40 kHz bandwidth of Ampex).

4.2 Transducer Calibration and System Linearity

The calibration data for the transducers supplied by the manufacturer were used to obtain the pressure. Several transducers were occasionally mounted together in an explosive charge driven shock tube to check the overall relative accuracy of these calibrations. This is discussed in Appendix B.

In spite of relatively reliable calibration data on the transducers, there will of course be errors introduced by the other components in the measuring chains. Some idea of these uncertainties can be estimated from the specifications given in Table 4.2.

5. DATA REDUCTION

5.1 Curve Tracing and A/D Conversion

In order to effectively analyse the pressure-time recordings, a D-mac curve-tracer was used to convert the analog signals to digital form. This is discussed in Appendix C. Further data reduction was performed on an IBM 370/155 and frontpressure (maximum average overpressure), impulse, positive duration and time of arrival were obtained. These data were then sorted according to test configuration, charge weight etc, and printed in tabular form /6/ and punched on cards for further analysis.

5.2 Fitting Technique for Scaling Relationships

For the 27 different model configurations described in Reports III and IV, a total of 2200 blast wave parameter values (peak pressure, impulse, and positive duration) were obtained. Attempts were made to fit these data to several equations based on various scaling relationships to link the data from these different configurations together. The type of equations tested did not permit the normal methods of least squares fitting and so an iterative procedure which requires no derivatives was used. This is discussed in more detail in Appendix D.

5.3 Electrical Filter for Chamber Pressure

As will be discussed in Report II, the recorded signals from the transducers mounted in the detonation chamber contained high frequency ringing. This was mainly due to the multiple reflected waves from the walls, but also to some extent due to vibrations of the chamber walls /31/. The signals from the magnetic tape were in this case passed through a carefully designed electrical filter used elsewhere /32/. There were, however, some alterations to the filter used in Ref.32 and a full description is therefore given in Appendix E.

REFERENCES

1. A. Skjeltorp, T. Hegdahl, and A. Jenssen, "Underground Ammunition Storage II A and II B Chamber Pressure" Technical note no 79/72, Norwegian Defence Construction Service (1975).

2. A. Skjeltorp, T. Hegdahl, and A. Jenssen, "Underground Ammunition Storage III A and III B: Single chamber storage with variable tunnel diameter and variable chamber volume". Technical note no 81/72, Norwegian Defence Construction Service (1975).

3. A. Skjeltorp, T. Hegdahl, and A. Jenssen, "Underground Ammunition Storage IV A and IV B: Connected chamber storage with variable chamber volume and variable angle between branch and main passageway". Technical note no 82/72, Norwegian Defence Construction Service (1975).

4. A. Skjeltorp, T. Hegdahl, and A. Jenssen, "Underground Ammunition Storage V A and V B: Connected chamber storage. Blast load on doors in two sites". Technical note no 83/72, Norwegian Defence Construction Service (1975).

5. Parts of the reports listed in Refs. 1-4 are published in Proceedings, Fourth International Symposium on the Military Applications of Blast Simulation, Atomic Weapons Research Establishment, Foulness, England (1974).

6. The reports in Refs. 1-4 labelled A contain the main results whereas the reports labelled B contain the raw data in the form of pressure-time recordings and tabulated blast wave parameters.

7. A. Jenssen, A. Sølvberg, H. Michalsen, "Sikerhetsspørsmål ved ammunisjonslagre". Fortifikatorisk notat 26/65. Norwegian Defence Construction Service, (1965).

8. A. Sølvberg, H. Michalsen, "Sikkerhetsspørsmål ved ammunisjonslagre. Trykkforhold i undergrunnslagre. Empiriske formler basert på modell-forsøk". Fortifikatorisk notat 27/65 Norwegian Defence Construction Service (1965).

9. A. Skjeltorp, A. Jenssen, "Underground Ammunition Storage Safety". Fortifikatorisk notat 32/66. Norwegian Defence Construction Service (1966).

10. A. Skjeltorp,
"Model tests to investigate external safety distances".
Fortifikatorisk notat 36/67.
Norwegian Defence Construction Service (1967).

11. A. Skjeltorp,
"One-dimensional blast wave propagation".
Fortifikatorisk notat 48/69.
Norwegian Defence Construction Service (1969).

12. G. Fredrikson and A. Jenssen,
"Underground Ammunition Storages. Model Tests to determine air blast propagation from accidental explosions".
Fortifikatorisk notat nr 59/70
Norwegian Defence Construction Service (1970).

13. This is being proposed as an improvement in the present determination of the hazardous area around an underground ammunition storage site as prescribed in Ref.14, which uses the net explosive quantity as basic input parameter.

14. NATO Safety Principles for the Storage of Ammunition and Explosives, NATO document AC/258-D/70, dated December 1969.

15. See for example W.E. Baker, P.S. Westine, and F.D. Dodge, "Similarity Methods in Engineering Dynamics" (Hyden Book Co., New Jersey, U.S.A., 1973) Ch. 4.

16. E. Strømsøe,
"Scaling of Underground Explosions and the Heat Loss Problem"
Teknisk notat VM-15
Norwegian Defence Research Establishment (1971).

17. This corresponds to a 200 m blast wave propagation in an exit tunnel with an average Mach number of 5.

18. R.G.S. Sewell, G.F. Kinney, and J.E. Sinclair,
"Internal Explosions in Vented and Unvented Chambers",
Minutes of the Fourteenth Explosives Safety Seminar,
Department of Defence Explosives Safety Board,
Washington D.C., p. 87 (1972).

19. This example is taken from an earlier test, Ref.12. These data are included in Report IV and represent one of the highest loading densities used in any of our tests.

20. D.R. Curran,
"Effects of an Explosion in an Underground Chamber",
Teknisk notat X-132
Norwegian Defence Research Establishment (1965).

21. A.T. Skjeltorp,
"Blast Wave Propagation in Rough-Walled Tunnels",
Fortifikatorisk notat nr 103/75,
Norwegian Defence Construction Service (1975).

22. A.R. Kribel,
"Airblast in Tunnels and Chambers",
Defence Nuclear Agency, Washington D.C. 20305
DASA 1200-11, Supplement 1 (1972).

23. E. Abrahamsson,
"Operation Block",
Proceedings Fourth International Symposium on Military Applications of Blast Simulation,
Atomic Weapons Research Establishment, Foulness, England (1974).

24. K.G. Schmidt,
"Underground Explosion Trials at Raufoss 1968: Blast Wave Propagation Following a Detonation in a Tunnel System",
Norwegian Defence Research Establishment,
Report no. X-128 (1970).

25. F.B. Porzel,
"Study of Schock Impedance Effects in a Rough Walled Tunnel",
Research Paper No. P-330, Institute for Defence Analysis,
AD 684790 (1969).

26. A. Rinnan, A.T. Skjeltorp, and A. Jenssen,
"Underground Ammunition Storage. Model Test to Investigate the Strength and Effectiveness of a Selfclosing Concrete Block",
Technical note no 98/73,
Norwegian Defence Construction Service, (1973).

27. For the present experiments the pressure unit is 1 bar and the ambient pressure is always set to p_o = 1 bar. In practice, therefore, $p = p_{so}$, which is consistent. The definition of p normally used in the present reports.

28. Eq. (2.4 f) was originally proposed by Emerich and Curtis in ref. 29 to describe the wall roughness attenuation.

29. R.J. Emerich and C.W. Curtis,
"Attenuation in Shock Tube",
J. Appl. Phys. 24, 360 (1953).

30. A.T. Skjeltorp and A. Jenssen,
"One-Dimensional Blast Wave Propagation",
Proceedings Fourth International Conference on Military Applications of Blast Simulation, Atomic Weapon Research Establishment, Foulness, England (1974).

31. The Kistler 603 B transducers have built in compensation for acceleration with a sensitivity of $< 10^{-4}$ bar/g.

32. C. Svensson,
"Metod för bestämning av toppvärde hos eksponentiellt förlopp med överlagrade svängningar",
Fortifikationsförvaltningen, Forskningsbyrån, Stockholm, C-rapport nr 52 (1972).

33. M.J.D. Powell,
"A method for minimizing sums of squares of non-linear functions without calculating derivatives",
Computer J, 7 , 303 (1965).

APPENDIX A

DEFINITIONS OF SYMBOLS

A Cross-sectional area defined as:
- A_j main passageway, single chamber storage site
- A_j' branch passageway, connected chamber storage site
- A_k main passageway, connected chamber storage site

c Velocity of sound

D = 4A/S, hydraulic diameter

E Elasticity module

E_c Conduction heat loss

E_D Deformation energy

E_t Total energy release of explosive

e Local height of wall roughness element

$\bar{e}$ Average height of wall roughness element

I Impulse (bar · ms)

k = $2 \in \bar{e}/D$, attenuation constant

L Distance along main passageway from:
- a) Chamber exit in single chamber storage sites
- b) Exit of branch passageway in connected chamber storage sites

n Linear scaling factor

p Peak overpressure (bar)

Q TNT charge weight

S Perimeter of cross-section of main passageway

t_+ Positive duration of pressure pulse

t_a Arrival time of shock front from time of detonation

v_m Angle between branch and main passageway

V Chamber volume (closed bomb)

V_i Chamber volume for single and connected chamber storage sites

V_t Total effective volume (Volume of chamber and tunnel system up to the observation point

$X_{\pm}$ Energy division factor for connected chamber storage sites

Y Impedance function

γ $= C_p/C_v$, specific heat ratio

ε Efficiency of feedback energy

λ_L Lamé's constant, def. in Fig. 2.3

μ_L Lamé's constant, def. in Fig. 2.3

μ $= (\gamma + 1)/(\gamma - 1)$

DEFINITION OF TERMS USED IN UNDERGROUND STORAGE

Adit: A passage or tunnel leading into an underground storage complex.
See Underground Storage

After-Burning: Blast or flames from post-detonation reaction between combustible explosion gases and ambient oxygen. This effect occurs for oxygen deficient explosives as for example T N T.
See Blast Wave, Jet-Effect

Average Overpressure: The pressure/time curve obtained by taking the mean values of the pressures of the peaks and troughs in a pressure oscillating system.

Average Peak overpressure: The maximum value of the average overpressure. See Average Overpressure

Ball of Fire (or Fireball): The luminous sphere of hot gases which forms a few millionths of a second after an explosion and immediately starts to expand and cool. The exterior of the ball of fire is initially sharply defined by the luminous shock front (in air) and later by the limits of the hot gases themselves. See Breakaway.

Blast Attenuation : The decrease in peak overpressure and/or impulse versus distance from the explosion source due to the rarefaction wave and/or due to energy dissipating effects in tunnel systems such as viscous loss due to wall roughness, thermal energy transmission to the walls, vertex formation etc.
See Rarefaction Wave, Viscous Loss, Wall Roughness, Vertex.

Blast Loading : The loading (or force) on an object caused by the air blast from an explosion striking and flowing around the object. It is a combination of overpressure (or diffraction) and dynamic pressure (or drag) loading.
See Diffraction, Drag, Dynamic Pressure, Overpressure.

Blast Protective Construction : Specifically designed building elements such as blast doors, blast valves etc. to reduce or prevent the entry into a chamber of the blast wave from the explosion of the contents of an adjacent chamber.
See Blast Door, Blast Valve, Blast Wave.

Blast Resisting Door : A door specifically designed to prevent the entry into a chamber of the gases, flame and air shock from the explosion of the contents of an adjacent chamber.

Blast Scaling Laws : Formulas which permit the calculation of the properties, e.g., overpressure, dynamic pressure, time of arrival, duration, etc.of a blast wave at any distance from an explosion of specified energy from the known variation with distance of these properties for a reference explosion of known energy, e.g. of 1 kilogram TNT.
See Cube Root Law.

Blast Trap : Special construction features in the tunnel system of an underground storage site such as turns, crossovers, obstacles, cross section changes etc., to reduce the blast wave leaving or entering a passageway.

Blast Valve : A valve in the ventilation system specifically designed to prevent the entry into a chamber of the blast wave from the explosion of the content of an adjacent chamber

Blast Wall : A wall which supports (or bears) part or mass of a structure, such as a blast door, specifically designed to withstand the blast wave from the explosion of the contents of an adjacent chamber.

Blast Wave : A pressure pulse of air, accompanied by winds, propagated continuously from an explosion.
See Shock wave.

Branch Passageway : The tunnel leading from the storage chamber to the main passageway in a connected chamber storage site.

Breakaway : The onset of a condition in which the shock front (in the air)moves away from the exterior of the expanding ball of fire produced by the explosion.
See Ball of fire, Shock front.

Bulk Velocity : The resultant velocity imparted to a mass by a series of shock and reflected waves.

Burst : Explosion or detonation.

Chamber Interval : The interval between the natural walls of adjacent underground storage sites.
See Quantity Distance

Chamber Storage Site : Normally a chamber excavated in a hill or a series of such chambers specially adapted for the storage of ammunition and explosives. A cavern may be structurally modified to be used as a chamber storage site.

Connected Chamber Storage Site : An excavated chamber which is inter-connected by air ducts or passageways to another storage chamber.

Contained Explosion : An explosion in an underground storage site with little or no venting to the surface.

Cover : The solid ground situated between the ceiling or wall of an underground chamber and the nearest exterior surface.

Crater : A hole or chasm in the overburden caused by a subterranean explosion.

Cube Root Law : A scaling law applicable to many blast phenomena. It relates the time and distance at which a given blast effect is observed to the cube root of the energy yield of the explosion.

Damage Criteria : Standards or measures used in estimating specific levels of damage.

Detonation. A violent chemical reaction within a chemical compound or mechanical mixture evolving heat and high pressures. A detonation, in contradistinction to deflagration, is the reaction which proceeds through the reacted material toward the unreacted material at a supersonic velocity. The result of the chemical reaction is an exertion of extremely high pressures on the surrounding medium forming a propagating shock wave which is originally of supersonic velocity. A detonation, when the material is located on or near the surface of the ground, is normally characterized by a crater.

Diffraction : The bending of waves around the edges of objects. In connection with a blast wave impinging on a structure, diffraction refers to the passage around and envelopment of the structure by the blast wave. Diffraction loading is the force (or loading) on the structure during the envelopment process.

Drag Loading : The force on an object or structure due to the transient winds accompanying the passage of a blast wave. The drag pressure is the product of the dynamic pressure and a coefficient which is dependent upon the shape (or geometry) of the structure or object.
See Dynamic pressure.

Dynamic Pressure : The air pressure which results from the mass air flow (or wind) behind the shock front of a blast wave. It is equal to the product of half the density of the air through which the blast wave passes and the square of the particle (or wind) velocity in the wave as it impinges on the object or structure.

Effective Net Explosive Quantity: See Net Explosive Quantity.

Elastic Range : The stress range in which a material will recover its original form when the force (or loading) is removed. Elastic deformation refers to dimensional changes occurring within the elastic range. See Plastic Range.

Emergent Shock or Blast : The shock wave issuing from an adit, a vent or a crater.

Explosion. The rapid production of hot gases at a high pressure as the result of a chemical reaction and the sudden release of this energy to cause strong dynamic stresses in the surroundings. The term usually relates to the effect of a detonation of initiating explosives and high explosives but applies in certain circumstances to the effect of a deflagration of propellant explosives.

Explosion Propagation : A process where the explosion in one chamber causes an explosion in an adjacent chamber due to blast, hot flames, or debris.

Explosive. A substance manufactured with a view to produce a practical effect by explosion or a pyrotechnic effect. An explosive atmosphere of gas, vapor or dust is not considered to be an explosive.

Exterior Quantity-Distance. The minimum permissible distance between a building or stack containing ammunition or explosives and a building or an assembly place or a public traffic route outside the explosives area.

Free Air Overpressure (or Free Air Pressure) : The unreflected pressure, in excess of the ambient atmospheric pressure, created in the air by the blast wave from an explosion.

Fullscale Trials : Detonation of large quantities of explosives (tons) in large scale installations in rock to simulate and observe the effects from possible accidental explosions.

Geometrical Copy Model Tests: Tests in a scaled down geometrically similar model of a full scale installation. The linear scales of the model are reduced by a scaling factor n, and the explosive charge weight by a factor of n^3 compared to the full scale installation.

Impulse: The product of the overpressure (or dynamic pressure) from the blast wave of an explosion and the time during which it acts at a given point. More specifically, it is the integral, with respect to time, of the overpressure (or dynamic pressure), the integration being between the time of arrival of the blast wave and that at which the overpressure (or dynamic pressure) returns to zero at the given point.

Interior Quantity-Distance. The minimum permissible distance between a building or stack containing ammunition or explosives and another such building or stack inside the explosives area.

Linear Scaling Factor : The ratio n between the linear dimension of a full scale installation and a geometrically similar model. The model tests are then said to be in a linear scale 1:n.

Loading : The force on an object or structure or element of a structure. The loading due to blast is equal to the net pressure in excess of the ambient value multiplied by the area of the loaded object etc.

Loading Density : The ratio Q/V, where Q is the total net explosive quantity and V is the volume of the confinement, e.g. a storage chamber.

Mach Front : See Mach Stem.

Mach Region : The region on the surface at which the Mach stem has formed as the result of a particular explosion in the air.

Mach Stem : The shock front formed by the fusion of the incident and reflected shock fronts from an explosion. The term is generally used with reference to a blast wave, propagated in the air, reflected at the surface of the earth. The Mach stem is nearly perpendicular to the reflecting surface and presents a slightly convex (forward) front. The Mach stem is also called the Mach front.
See Shock front, Shock wave.

Main Passageway : A passage or tunnel leading into an underground storage complex.

Mass Explosion. An explosion which affects almost instantaneously the entire quantity of explosives under consideration. The term usually relates to detonation but also applies to deflagration when the practical effects are similar, for example the mass deflagration of propellant under very strong confinement so as to produce a bursting effect and a serious hazard from debris.

Model Tests : See Geometrical Copy Model Tests

Net Explosives Quantity. The net explosives quantity is the total explosives contents of ammunition unless it has been determined that the effective quantity is significantly different from the actual quantity. It does not include such substances as white phosphorous, war gases or smoke and incendiary compositions unless these substances contribute significantly to the dominant hazard of the hazard division concerned.

Overhead Cover : See Cover

Overpressure : The transient pressure, usually expressed in bars or pounds per square inch exceeding the ambient pressure, manifested in the shock (or blast) wave from an explosion. The variation of the overpressure with time depends on the energy yield of the explosion, the distance from the point of burst, and the medium in which the explosive is detonated. The peak overpressure is the maximum value of the overpressure at a given location and is generally experienced at the instant the shock (or blast) wave reaches that location.
See Shock wave.

Particle Velocity : The local velocity imparted by the transmission of a shock or a reflected wave.

Peak Overpressure : See Overpressure.

Plastic Range : The stress range in which a material will not fail when subjected to the action of a force, but will not recover completely, so that a permanent deformation results, when the force is removed. Plastic deformation refers to dimensional changes occurring within the plastic range. See : Elastic range.

Positive Phase : See Shock Wave.

Propagation by Hot Gases : See Explosion Propagation.

Propagation by Rock Spall : See Explosion Propagation.

Quantity-Distance. The minimum permissible distance between a building or stack containing a given quantity of ammunition or explosives and any other exposed structure, assembly place or traffic route. It is based on an acceptable risk to life and property from the effects of a mass fire or an explosion.

Rarefaction Wave : An underpressure pulse produced as the blast wave emerges from the open end of a duct and travels back into the duct increasing the normal pressure decay.

Reflection Factor : The ratio of the total (reflected) pressure to the incident pressure when a shock (or blast) wave travelling in one medium strikes another.

Reflected Pressure : The total pressure which results instantaneously at the surface when a shock (or blast) wave travelling in one medium strikes another medium, e.g., at the instant when the front of a blast wave in air strikes the surface of an object or structure.

Reverberations : The pressure oscillations produced in a confined space by the transit of shocks and reflected shocks in the gases.

Scaling Factor : See Linear Scaling Factor.

Scaling Law: A mathematical relationship which permits the effects of an explosion of given energy yield to be determined as a function of distance from the explosion, provided the corresponding effect is known as a function of distance for a reference explosion, e.g. 1 kg TNT. See Blast scaling law, Cube root law.

Secondary Peaks : The highest pressure recorded in the transmission of each of a series of reflected shocks following the initial shock and its primary reflected shock.

Shock Front (or Pressure Front) : The fairly sharp boundary between the pressure disturbance created by an explosion (in air, water or earth) and the ambient atmosphere, water or earth respectively. It constitutes the front of the shock (or blast) wave.

Shock Wave : A continuously propagated pressure pulse (or wave) in the surrounding medium which may be air, water or earth initiated by the expansion of the hot gases produced in an explosion. A shock wave in air is generally referred to as a blast wave, because it is similar to (and is accompanied by) strong, but transient, winds. The duration of a shock (or blast) wave is distinguished by two phases. First there is the positive (or compression) phase during which the pressure rises very sharply to a value that is higher than ambient and then decreases rapidly to the ambient pressure. The duration of the positive phase increases and the maximum (peak) pressure decreases with increasing distance from an explosion of given energy yield. In the second phase, the negative (or suction) phase, the pressure falls below ambient and then returns to the ambient value. The duration of the negative phase is approximately constant throughout the blast wave history and may be several times the duration of the positive phase. Deviations from the ambient pressure during the negative phase are never large and they decrease with increasing distance from the explosion.
See : Overpressure.

Single Chamber Storage Site : An excavated chamber which has its own entrance from the exterior and is not connected by air ducts or passageways to any other storage chamber.

Site. Any cavern, chamber, building, cell or stack which contains ammunition and/or explosives.

Specific Impulse : The impulse per unit area.

Static Pressure : See Overpressure.

Storage Chamber : An excavated chamber in rock used for storage of explosives and ammunition.

Thermal Energy: The energy emitted from the ball of fire as thermal radiation. The total amount of thermal energy received per unit area at a specified distance from a nuclear (or atomic) explosion is generally expressed in terms of calories per square centimeter.

TNT Equivalent: A measure of the energy released in the detonation of ammunition or explosives of a given quantity expressed in terms of the quantity of TNT which would release the same amount of energy when exploded. The TNT equivalent is usually stated in kilograms or tons. The basis of the TNT equivalence is that the explosion of 1 ton of TNT releases 10^9 calories of energy.

Uncontained Explosion : An explosion taking place in open air or on a free surface.

Underground Explosion : The explosion of explosives or ammunition with its centre beneath the surface of the ground.

Underground Storage. Storage in a cavern or chamber storage site with a ceiling more than 60 cm below the natural ground level and storage in a site tunnelled into a hill.

Underground Storage Site : A cavern or chamber storage site with a ceiling not less than 60 cm below the natural ground level, specially adapted for the storage of ammunition and explosives.

Venting : The reduction of pressure in a chamber or storage complex due to the release of gases into a corridor, another chamber, through an adit or through an aperture in the overburden.

Vortex: A turbulent movement of gas produced by blast waves passing constrictions, corners, exits, etc.

Viscous Loss : A reduction in peak pressure at the shock front which results from the roughness of tunnel or tube walls.

Wall Roughness : The average height of the irregularities of the wall of a tube or tunnel.

APPENDIX B

CALIBRATION OF PRESSURE TRANSDUCERS AND MEASURING CHAIN

The purpose of the calibration was to check the pressure transducers and to find the errors introduced by the total signal processing chain and digitizing system. Fig. B.1 shows the explosive charge (TNT) driven shock tube used in the calibration. Six pressure transducers were mounted head on at one end of the tube on a circle around the centreline of the tube. The transducers were also heat protected from the detonation gases by a layer of silicon grease.

The measuring chain was as shown in Fig. 4.1 c (Mode A), and the pressure-time recordings were digitized as discussed in Appendix C. The peak pressure, impulse and positive duration as well as mean standard deviations were found employing special computer programmes, Appendix C. The calibration data supplied by the manufacturer were used in these calculations. Two sets of six transducers were listed, one set with serial number and higher numbers.

The results are shown in Table B.1. As may be seen, the mean standard deviation for peak pressure was about 4% and for impulse about 8%.

During the course of the experiments to be discussed in the following reports, occasional checks of this type showed that the transducer calibrations remained remarkably constant ($\pm$ 5%). There were a few instances where one transducer would suddenly fail, but this could easily be detected from the grossly erroneous pressure data and certain characteristics in the total pressure-time history (noise, discharge patters).

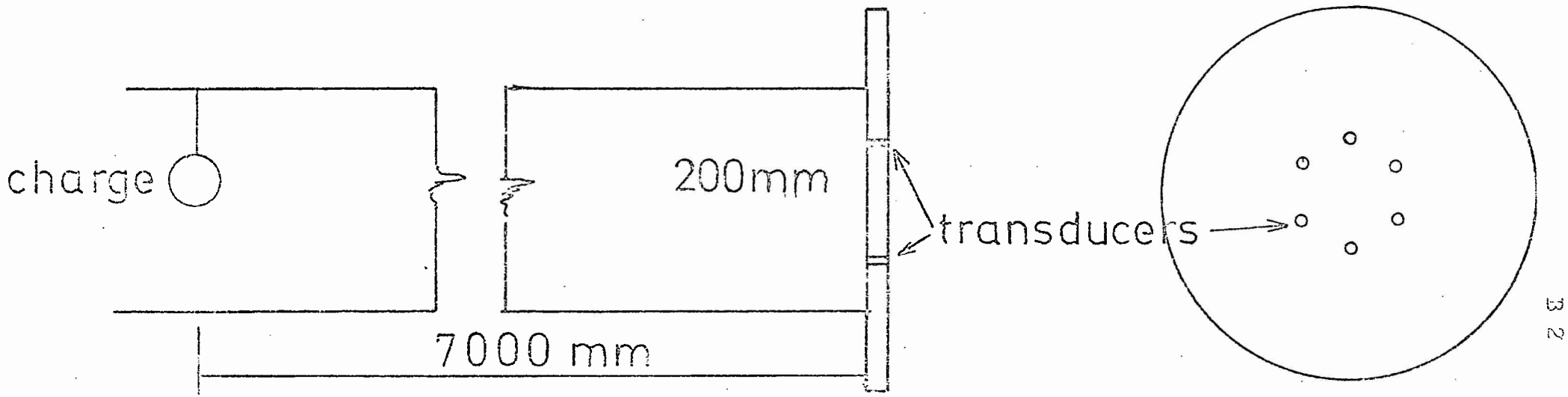

FIG. B1 Tube for calibration.

Table B.1

CALIBRATION OF PRESSURE-TRANSDUCERS APRIL 1971
STRAIGHT TUBE, LENGTH 7 METER. DIAMETER 200 MM

CHARGE (GRAMS)	DISTAN. (METRE)	PEAK PRES. (BAR)	AVER. PEAK-PRES.(BAR)	DEVIAT. (%)	IMPULSE (BAR*MSEC)	AVER. IMP. (BAR*MSEC)	DEVIATION (%)	POS. DURAT. (MSEC)	IDENTIFI.
17.5	7.00	4.925	4.905	1.6	12.651	12.615	0.3	7.30	8047101.
17.5	7.00	5.021	4.905	2.4	13.255	12.615	5.1	8.15	8047102.
17.5	7.00	4.946	4.905	1.2	13.116	12.615	4.0	7.94	8047103.
17.5	7.00	5.029	4.905	2.5	13.276	12.615	5.2	8.25	8047104.
17.5	7.00	4.892	4.905	2.1	10.776	12.615	14.6	7.65	8047106.
17.5	7.00	4.480	4.476	0.1	11.917	11.613	2.6	7.65	18047103.
17.5	7.00	4.472	4.476	0.1	11.309	11.613	2.6	7.22	18047104.
17.5	7.00	4.776	4.808	0.7	13.584	12.473	8.9	8.09	19047111.
17.5	7.00	4.841	4.808	3.5	12.385	12.473	0.7	7.25	19047112.
17.5	7.00	4.860	4.808	1.1	12.689	12.473	1.7	8.10	19047103.
17.5	7.00	4.875	4.808	1.4	12.212	12.473	2.1	6.89	19047104.
17.5	7.00	4.936	4.808	1.6	11.498	12.473	7.8	6.99	19047126.
20.0	7.00	5.771	6.073	5.0	16.234	17.096	5.0	8.59	3047101.
20.0	7.00	6.241	6.073	2.8	18.919	17.096	10.7	12.14	3047102.
20.0	7.00	6.114	6.073	0.7	15.763	17.096	7.8	7.90	3047103.
20.0	7.00	6.165	6.073	1.5	17.469	17.096	2.2	9.96	3047104.
25.5	7.00	6.392	6.605	3.2	15.853	16.481	3.8	7.24	9047101.
25.5	7.00	7.113	6.605	7.7	17.713	16.481	7.5	8.63	9047102.
25.5	7.00	6.838	6.605	3.5	17.230	16.481	4.5	8.44	9047103.
25.5	7.00	6.872	6.605	4.0	16.677	16.481	1.2	8.16	9047104.
25.5	7.00	6.999	6.605	7.7	17.933	16.481	8.8	11.23	9047115.
25.5	7.00	6.813	6.605	4.4	13.479	16.481	18.2	7.24	9047116.
25.5	7.00	6.276	6.178	1.6	16.297	15.957	2.1	8.47	10047102.
25.5	7.00	6.325	6.178	2.4	16.287	15.957	2.1	7.84	10047103.
25.5	7.00	6.202	6.178	0.4	16.350	15.957	2.5	8.49	10047104.
25.5	7.00	5.946	6.178	5.4	15.817	15.957	0.9	9.79	10047105.
25.5	7.00	6.242	6.178	1.0	15.034	15.957	5.8	8.39	10047106.

CALIBRATION OF PRESSURE-TRANSDUCERS APRIL 1971
STRAIGHT TUBE, LENGTH 7 METER. DIAMETER 200 MM

Table B.1

CHARGE (GRAMS)	DISTAN. (METRE)	PEAK PRES. (BAR)	AVER. PEAK-PRES.(BAR)	DEVIAT. (%)	IMPULSE (BAR*MSEC)	AVER. IMP. (BAR*MSEC)	DEVIATION (%)	POS. DURAT. (MSEC)	IDENTIFI.
9.5	7.00	2.532	2.590	2.2	6.961	7.124	2.3	7.20	7047101.
9.5	7.00	2.444	2.590	2.1	7.761	7.124	8.9	7.51	7047102.
9.5	7.00	2.562	2.590	1.1	6.895	7.124	3.2	7.09	7047103.
9.5	7.00	2.555	2.590	1.4	6.587	7.124	7.5	7.29	7047104.
9.5	7.00	2.658	2.590	2.6	7.414	7.124	4.1	7.29	7047106.
9.5	7.00	2.703	2.808	3.8	7.644	7.584	0.8	7.37	15047111.
9.5	7.00	2.761	2.808	1.7	7.491	7.584	1.2	7.51	15047112.
9.5	7.00	2.878	2.808	2.5	7.679	7.584	1.2	7.35	15047103.
9.5	7.00	2.890	2.808	2.9	7.523	7.584	0.8	7.24	15047104.
9.5	7.00	2.723	2.754	1.1	6.567	6.599	0.5	6.79	16047111.
9.5	7.00	2.709	2.754	1.6	7.430	6.599	12.6	7.66	16047112.
9.5	7.00	2.704	2.754	1.5	4.895	6.599	25.8	7.31	16047103.
9.5	7.00	2.790	2.754	1.3	7.505	6.599	13.7	7.51	16047104.
9.5	7.00	2.605	2.708	3.8	7.581	7.707	1.6	6.96	17047111.
9.5	7.00	2.736	2.708	1.0	7.736	7.707	0.4	8.24	17047112.
9.5	7.00	2.722	2.708	0.5	7.054	7.707	8.5	7.17	17047103.
9.5	7.00	2.769	2.708	2.3	8.459	7.707	9.8	7.34	17047104.
10.0	7.00	2.092	2.148	2.6	5.610	6.113	8.2	6.65	2047101.
10.0	7.00	2.147	2.148	0.0	6.655	6.113	8.9	7.52	2047102.
10.0	7.00	2.150	2.148	0.1	6.023	6.113	1.5	6.72	2047103.
10.0	7.00	2.203	2.148	2.6	6.165	6.113	0.8	7.09	2047104.
17.5	7.00	4.419	4.375	1.0	7.781	10.834	28.2	8.11	6047101.
17.5	7.00	4.408	4.375	0.7	11.846	10.834	9.3	7.42	6047102.
17.5	7.00	4.289	4.375	2.0	11.647	10.834	7.5	8.07	6047103.
17.5	7.00	4.315	4.375	1.4	10.680	10.834	1.4	6.89	6047104.
17.5	7.00	4.446	4.375	1.6	12.217	10.834	12.8	7.41	6047106.

Table B.1

CALIBRATION OF PRESSURE-TRANSDUCERS APRIL 1971
STRAIGHT TUBE, LENGTH 7 METER. DIAMETER 200 MM

CHARGE (GRAMS)	DISTAN. (METRE)	PEAK PRES. (BAR)	AVER. PEAK-PRES.(BAR)	DEVIAT. (%)	IMPULSE (BAR*MSEC)	AVER. IMP. (BAR*MSEC)	DEVIATION (%)	POS. DURAT. (MSEC)	IDENTIFI.
1.5	7.00	0.796	0.822	3.2	1.659	1.725	3.8	4.97	1047101.
1.5	7.00	0.806	0.822	1.9	1.848	1.725	7.1	4.94	1047102.
1.5	7.00	0.823	0.822	0.2	1.689	1.725	2.1	4.63	1047103.
1.5	7.00	0.861	0.822	4.8	1.705	1.725	1.2	4.56	1047104.
1.5	7.00	0.799	0.804	0.6	1.691	1.661	1.8	4.86	4047101.
1.5	7.00	0.807	0.804	0.3	1.705	1.661	2.6	4.86	4047102.
1.5	7.00	0.794	0.804	1.3	1.605	1.661	3.3	4.79	4047103.
1.5	7.00	0.817	0.804	1.6	1.643	1.661	1.1	4.77	4047104.
1.5	7.00	0.681	0.701	2.8	1.325	1.354	2.2	4.40	13047111.
1.5	7.00	0.698	0.701	0.4	1.347	1.354	0.5	4.54	13047112.
1.5	7.00	0.713	0.701	1.7	1.347	1.354	0.5	4.50	13047103.
1.5	7.00	0.733	0.701	4.7	1.415	1.354	4.5	4.40	13047104.
1.5	7.00	0.678	0.701	3.2	1.338	1.354	1.2	4.92	13047125.
1.5	7.00	0.793	0.820	3.2	1.694	1.682	0.7	4.99	14047111.
1.5	7.00	0.804	0.820	1.9	1.746	1.682	3.8	5.20	14047112.
1.5	7.00	0.818	0.820	0.2	1.658	1.682	1.5	4.81	14047103.
1.5	7.00	0.836	0.820	2.0	1.529	1.682	9.1	4.50	14047104.
1.5	7.00	0.846	0.820	3.3	1.785	1.682	6.1	4.96	14047125.
9.5	7.00	2.462	2.507	1.8	6.695	6.770	1.1	7.02	5047101.
9.5	7.00	2.498	2.507	0.4	6.564	6.770	3.0	7.13	5047102.
9.5	7.00	2.507	2.507	0.0	6.903	6.770	2.0	7.35	5047103.
9.5	7.00	2.460	2.507	1.9	6.571	6.770	2.9	6.98	5047104.
9.5	7.00	2.409	2.507	4.1	7.119	6.770	5.2	7.73	5047106.

Table B.1

CALIBRATION OF PRESSURE-TRANSDUCERS APRIL 1971
STRAIGHT TUBE, LENGTH 7 METER. DIAMETER 200 MM

CHARGE (GRAMS)	DISTAN. (METRE)	PEAK PRES. (BAR)	AVER. PEAK-PRES.(BAR)	DEVIAT. (%)	IMPULSE (BAR*MSEC)	AVER. IMP. (BAR*MSEC)	DEVIATION (%)	POS. DURAT. (MSEC)	IDENTIFI.
25.5	7.00	7.279	7.472	2.6	20.196	19.337	4.4	8.37	20047111.
25.5	7.00	7.479	7.472	0.1	21.039	19.337	8.8	12.38	20047112.
25.5	7.00	7.559	7.472	1.2	20.431	19.337	5.7	8.93	20047103.
25.5	7.00	7.530	7.472	0.8	18.858	19.337	2.5	8.81	20047104.
25.5	7.00	7.514	7.472	0.6	16.163	19.337	16.4	7.52	20047126.
51.5	7.00	12.046	12.179	1.1	26.972	27.565	2.2	8.07	11047101.
51.5	7.00	12.275	12.179	0.8	27.139	27.565	1.5	7.71	11047102.
51.5	7.00	12.066	12.179	0.9	25.799	27.565	6.4	7.56	11047103.
51.5	7.00	12.159	12.179	0.2	25.671	27.565	6.9	7.78	11047104.
51.5	7.00	12.346	12.179	1.4	27.902	27.565	1.2	8.90	11047105.
51.5	7.00	12.183	12.179	0.0	31.906	27.565	15.7	10.42	11047106.
51.5	7.00	13.354	13.912	4.0	28.256	30.000	5.8	7.67	12047101.
51.5	7.00	13.814	13.912	0.7	31.274	30.000	4.2	8.74	12047102.
51.5	7.00	13.414	13.912	3.6	29.323	30.000	2.3	8.97	12047103.
51.5	7.00	13.593	13.912	2.4	32.187	30.000	7.3	10.74	12047104.
51.5	7.00	14.171	13.912	3.3	31.846	30.000	6.2	10.08	12047105.
51.5	7.00	14.938	13.912	7.4	27.112	30.000	9.6	8.06	12047106.

STANDARD DEVIATION FOR PRESSURE (% DEVIATION FROM MEAN VALUE) 3.1

STANDARD DEVIATION FOR IMPULS (% DEVIATION FROM MEAN VALUE) 7.6

APPENDIX C

DATA REDUCTION

The pressure-time recordings were displayed in analog form either on Polaroid plates or UV sensitive paper (Sec. 4.1), which were not suitable for further analysis. The analog signals were therefore converted into digital form using a D-mac curve tracer. The procedure is outlined in Fig. C.1, where a relatively small number of discrete points on the curve reproduces the essential features of the pressure-time history. The curve tracer then simply converts the x, y coordinates for each of these points to voltages, which are digitized using an analog-to-digital converter. In practice up to approximately 60 points on each curve digitized. In addition, a total of five fixed points (1 - 5 in Fig. C.1) were digitized to give the pressure unit (pts 1-2) and time unit (pts 2-3). Points 4 and 5 were used to establish the zero-pressure line (x-axis).

The digital data characterizing each recording, were subsequently proeessed on an IBM 370/155 computer and four parameters were determined employing special computer programmes:

- Peak pressure (p): The maximum value of the pressure-time curve obtained by taking the mean values of the pressure oscillating system
- Impulse (I): The sum of trapezoids between the x-axis and pairs of successive digitized points on the curve located above the zero over-pressure line (x-axis)
- Positive duration (t_+): The time difference between the arrival of the shock front (point 5 in Fig. C.1) and the crossing of the smoothed curve with the zero over-pressure line (x-axis)
- Arrival time (t_a): The time difference between the recordings of the shock fronts in the detonation chamber and the actual measuring point.

These parameters were then sorted according to test configuration, charge weight etc. and stored for further analysis.

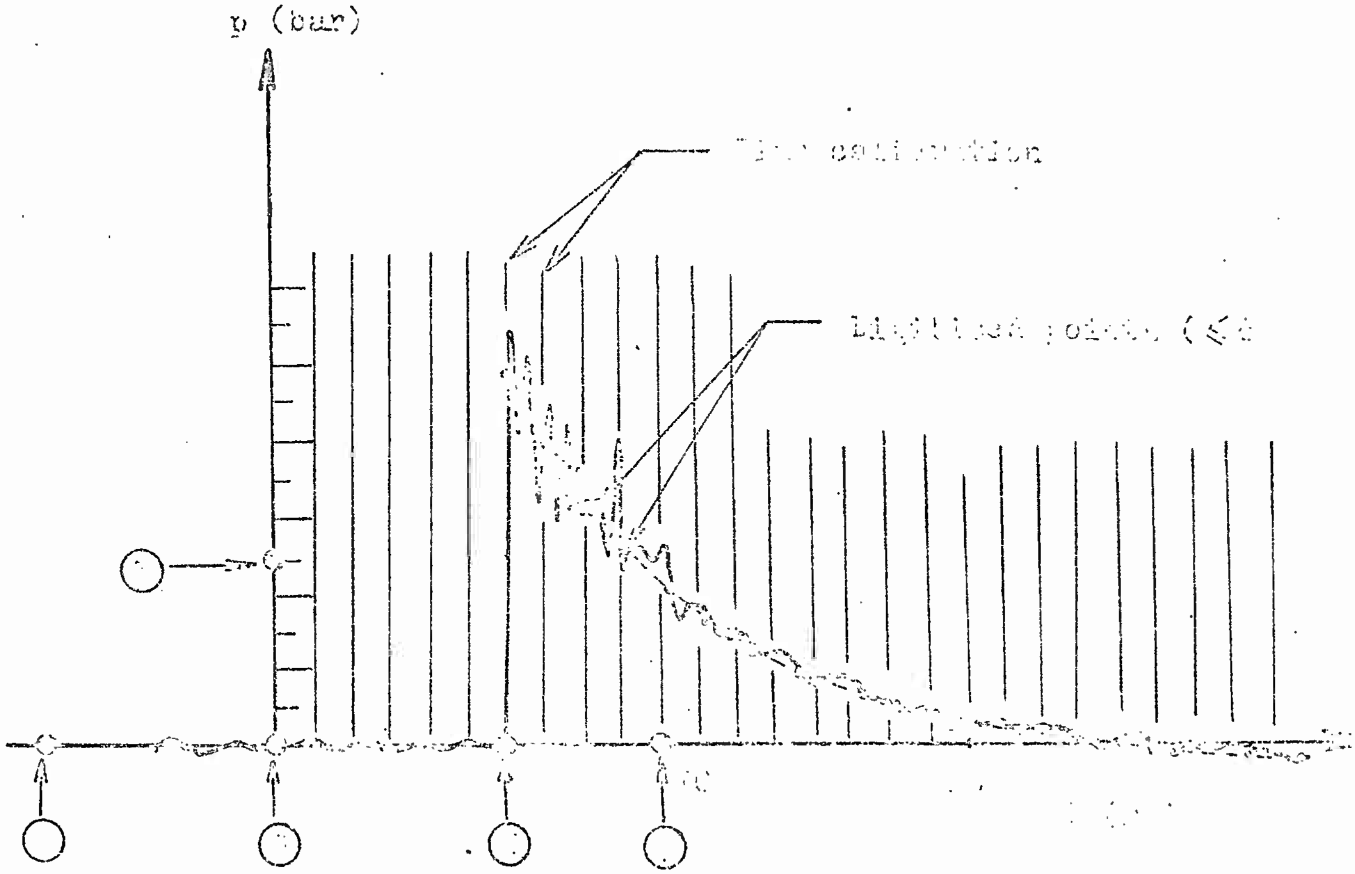

Fig. C.1: [illegible]

APPENDIX D

FITTING TECHNIQUES TO ESTABLISH SCALING RELATIONSHIPS

This appendix has been included in order to outline a special fitting technique used in Reports III and IV, to probe various empirical scaling relationships and obtain a consistent set of scaling parameters. This technique, originally proposed by Powell /33/, follows the normal least squares fitting routine up to certain point.

Let x_i, y_i be the observed data to be fitted to $y = f(x, a_1, b, c, ...)$, where f is a function described by the parameters a, b, c, ... If the calculated value of y is given by $y_i = f(x_i, a, b, c \ ...)$, the aim of the usual least squares fit is to minimize $L = \sum_i (y_i - y_i)^2$:

$$\frac{\partial L}{\partial a} = \frac{\partial L}{\partial b} = \frac{\partial L}{\partial c} = ... = 0 \qquad (D.1)$$

In the least squares fitting procedure, these equations are solved to give the best fit values of a, b, c, ... However, the function f(x, a, b, c, ...) may be so complex that Eqs.(D.1) cannot be solved in a straightforward way.

In this case one can use a method which in essence approximates the derivatives by differences through an iterative procedure /33/.

In practice this iterative fitting procedure was carried out using an IBM 370/155 computer and the programme was written to be able to fit up to nine parameters, but actually no more than four were used in the present work. The programme also produced standard errors on the fitted coefficients as well as their correlations.

APPENDIX E

FILTER TECHNIQUE FOR DETERMINATION OF MAXIMUM AVERAGE PRESSURE

This appendix describes the use and construction of two RC-filters to produce the maximum value of an exponentially decaying signal containing severe noise or ringing. The technique is based on earlier work by C. Swensson at the Royal Swedish Fortification Administration /32/, but with minor changes which warrants the description here.

The filter technique was used to obtain an unambigous interpretation of the pressure-time recordings in the detonation chamber (Report II). These recordings were characterized by high frequency ringing due to the multiple reflected waves from the chamber walls superimposed on an approximately exponential pressure decay.

The high frequency ringing can be filtered out, but then the maximum average pressure is also reduced. As will be discussed, it is possible to restore the true average maximum pressure by using two different filterfrequences and appropriate correction factors.

Fig. E.1 shows the principle for the experimental set-up. The unfiltered recorded signal is fed through two-pole RC-filters with different cut-off frequencies $f_1 = 2\pi/R_1C_1$ and $f_2 = 2\pi/R_2C_2$, and displayed on an UV writer. The unfiltered signal is also displayed for comparison.

In practice, the RC-filter in Fig.E.1 consists of four filters in series of the type shown in Fig.E.2. The four RC-filters are isolated from each other, using an operational amplifier of AD 741 CH the type as a voltage follower with an input impedance of 2 Mohm.

The following components were chosen:

Filter no j	R_j (kΩ)	C_j (μF)	-3dB frequency= $f_j=1/R_jC_j$ (Hz)
1	10	1	15,85
2	20	1	7,96

With four filters of these types in series the response function has a -12 dB/octave high frequency roll-off.

The filters were applied to the playback signals from the Ampex tape recorder. The tape speed as the signals were recorded, was 60 in per sec and the playback speed was 1 7/8 in per sec. This means a factor of 32 reduction in frequency from the real time frequencies which justifies the use of the rather low filter frequencies in the preceding table.

In order to calculate the response functions at a and b in Fig.E.1 of the two filtered signals, a Laplace transformation is used. The unfiltered signal is assumed to be of form

$$p(t) = p_o e^{-\tau/t} + n(t), \qquad (E.1)$$

where n(t) represents the superimposed noise as a function of time. The noise is assumed to be of such high frequency that it will be removed by the two filters. The response function of the four series-coupled circuits in Fig.E.2 is then

$$R(s) = \left(\prod_{i=1}^{4} \frac{\frac{1}{R_i C_i}}{S + \frac{1}{R_i C_i}}\right) \frac{p_o}{S + \tau} \qquad (E.2)$$

where $R_i C_i$ is the time constant for the ith stage ($R_1C_1 = R_2C_2 = R_3C_3 = R_4C_3 = RC$).
The inverse Laplace-transformation produces two cases for the response function in the time domain:

$\underline{R_j C_j = \tau}$:

$$p_j(t) = p_o \left(\frac{1}{R_j C_j}\right)^4 \frac{1}{24} t^4 e^{-\frac{t}{R_j C_j}} \qquad (E.3)$$

j = 1 or 2 corresponds to filter 1 or 2 in Fig.E.1.

$R_jC_j \neq \tau$:

$$p_j(t) = p_o\left(\frac{1}{R_jC_j}\right)^4 \left\{\exp\left(-t/R_jC_j\right)\left[\frac{t^3}{6(\tau - 1+R_jC_j)} - \frac{t^2}{2(\tau - 1/R_jC_j)^2}\right.\right.$$

$$\left. + \frac{t}{(\tau - 1/R_jC_j)^3} - \frac{1}{(\tau - 1/R_jC_j)^4}\right]$$

$$\left. + \exp(-\tau/t)\ \frac{1}{(\tau - 1/R_jC_j)^4}\right\} \qquad \text{(E.4)}$$

If A and B are the maximum values of the filtered signals in Fig.E.1, then from Eq.(E.3) or (E.4):

$$A = p_1(t = \sigma\tau)$$

$$B = p_2(t = \sigma\tau) \qquad \text{(E.5)}$$

By convention we shall assume A > B which is consistent with the present filter frequencies. Clearly, $A < p_o$ and $B < p_o$ and it is convenient to introduce two correction factors k_1 and k_2 defined as:

$$k_1 = \frac{p_o}{A} - 1$$

$$k_2 = \frac{p_o}{B} - 1 \qquad \text{(E.6)}$$

from which

$$p_o = \frac{k_2/k_1 - 1}{k_2/k_1 - A/B}\, A = KA \qquad \text{(E.7)}$$

where

$$K = \frac{k_2/k_1 - 1}{k_2/k_1 - A/B} \qquad \text{(E.8)}$$

With the present filter frequencies, Fig. E.3 shows K as a function A/B.

As an illustration, Fig.E.4 shows the filtered signals from an actual experiment. The ratio between the amplitude of the two filtered signals is found to be

$$A/B = 1,02$$

Now, turning to Fig.E.3, this value for A/B produces a correction factor

$$K = 1,025$$

The true maximum average pressure p_o can now be found from Eq.(E.7) as:

$$p_o = K \cdot A = 1,025 \times 4,0 = 4,1 \text{ bar}$$

The adequateness of this whole procedure was checked by varying the filter frequencies f_1 and f_2 over a relatively wide range. The calculated values for p_o appeared to be reproducible within approximately 5 - 10%. An increased uncertainty was observed for signals which deviated from the ideal exponential pressure decay in Eq.(E.1).

Essentially the same procedure can be followed to estimate the positive impulse

$$I = \int_o^\infty p_o \, e^{-\tau/t} \, dt = p_o/\tau \, ,$$

but this was not used in the present experiments.

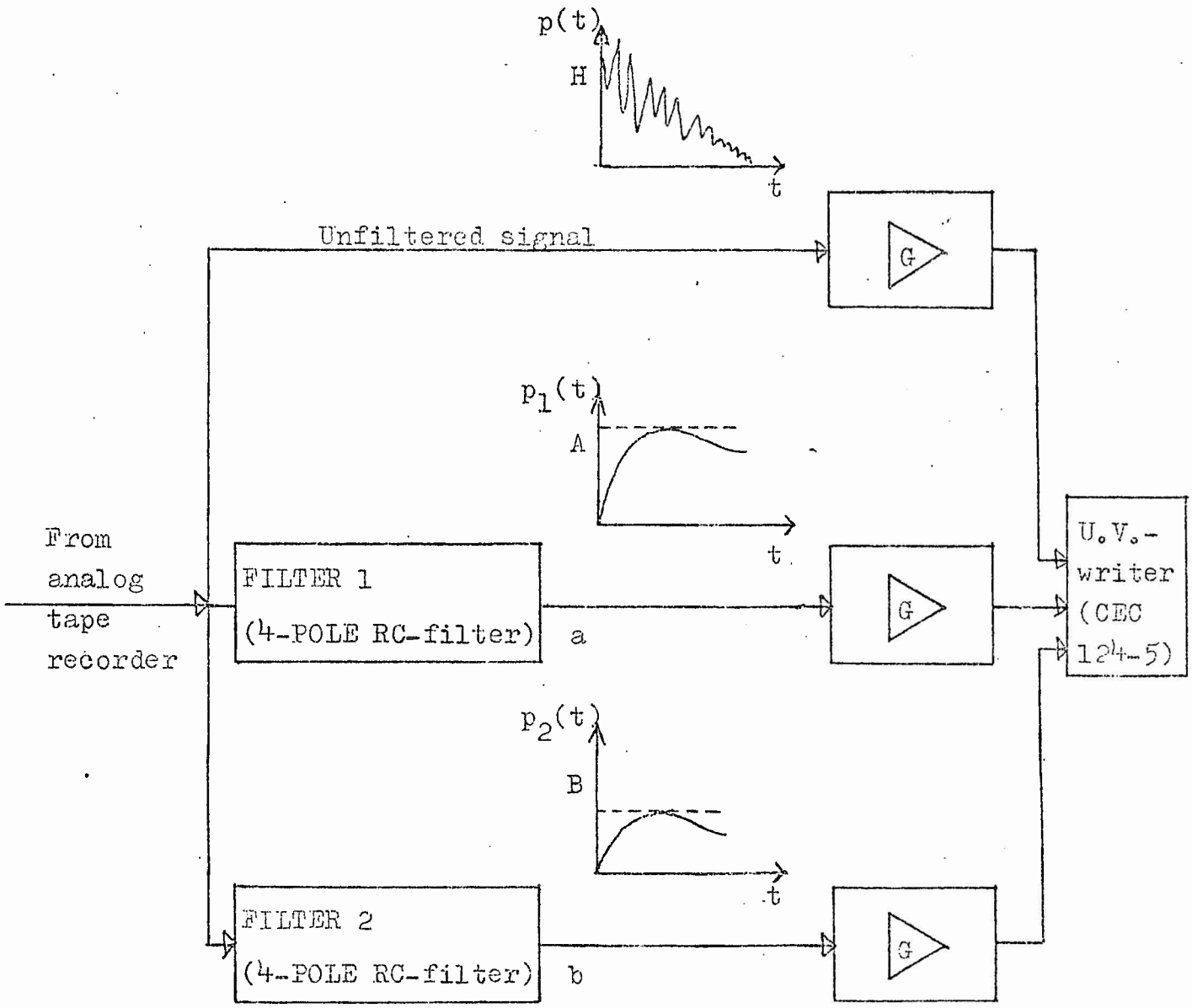

G = galvanometer amplifiers
(Kistler 5211)

Fig.E.1: Block diagram of the electronics used to filter the chamber pressure measurements. Details of Filter 1 and 2 are shown in Fig.E.2.

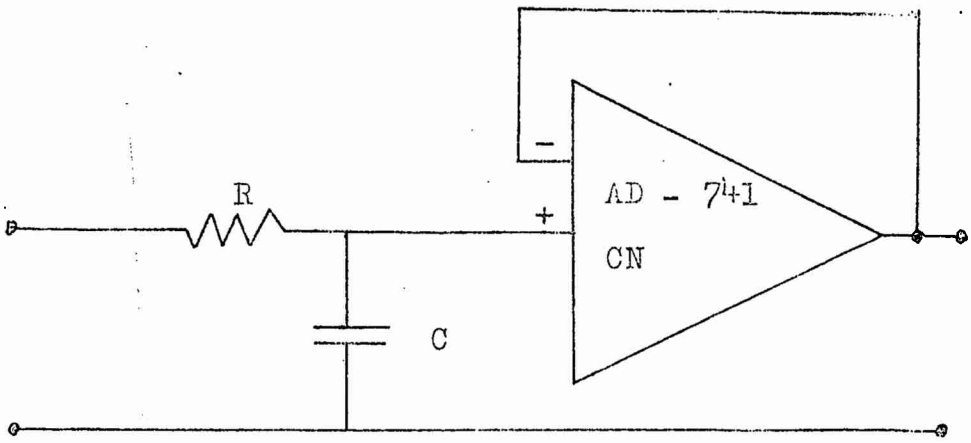

Fig.E.2: Filters 1 and 2 in Fig.E.1 consist of four circuits of this type placed in series. The operational amplifier serves to isolate the four RC-filters.

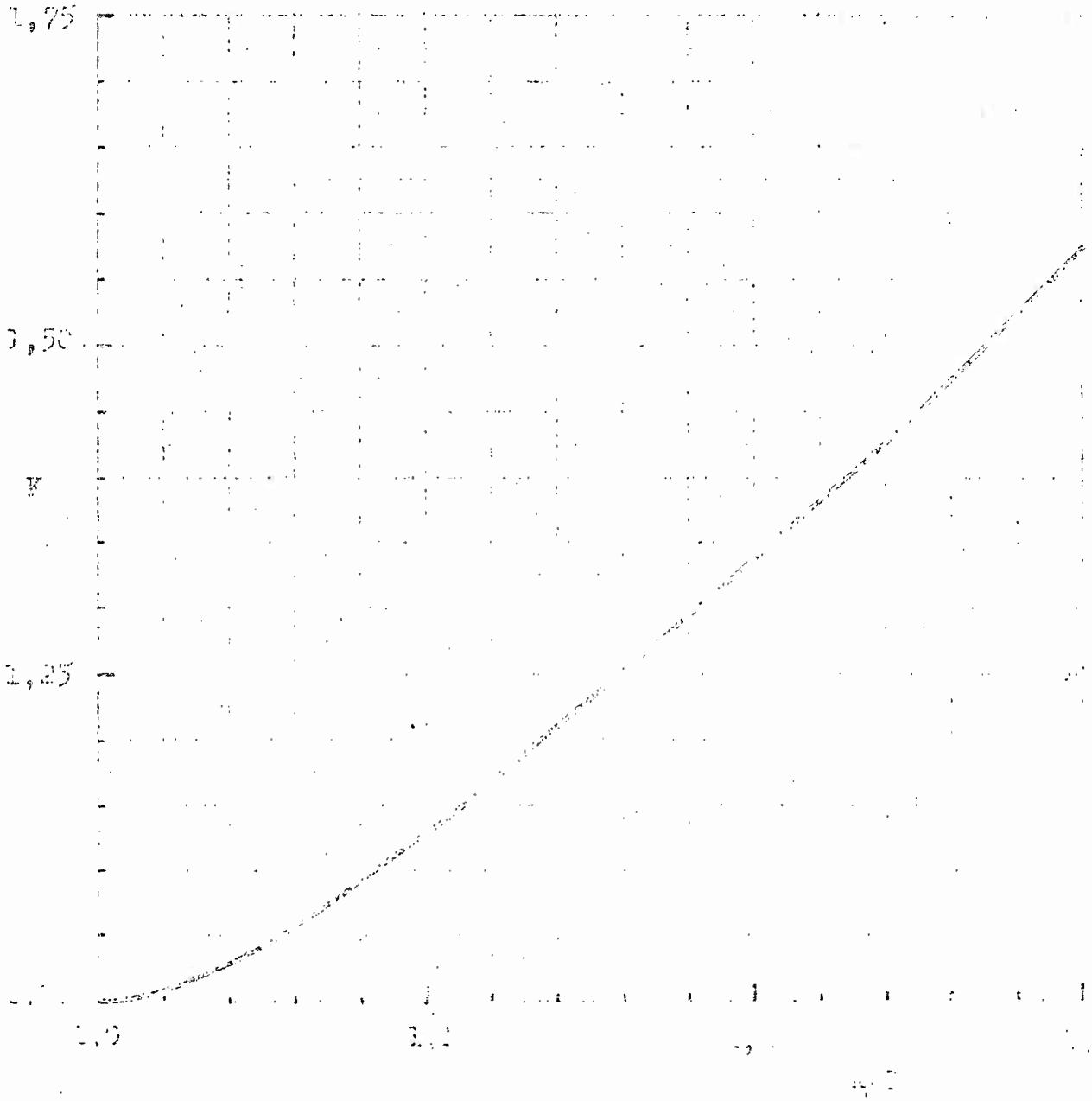

FIG E.3. Correction

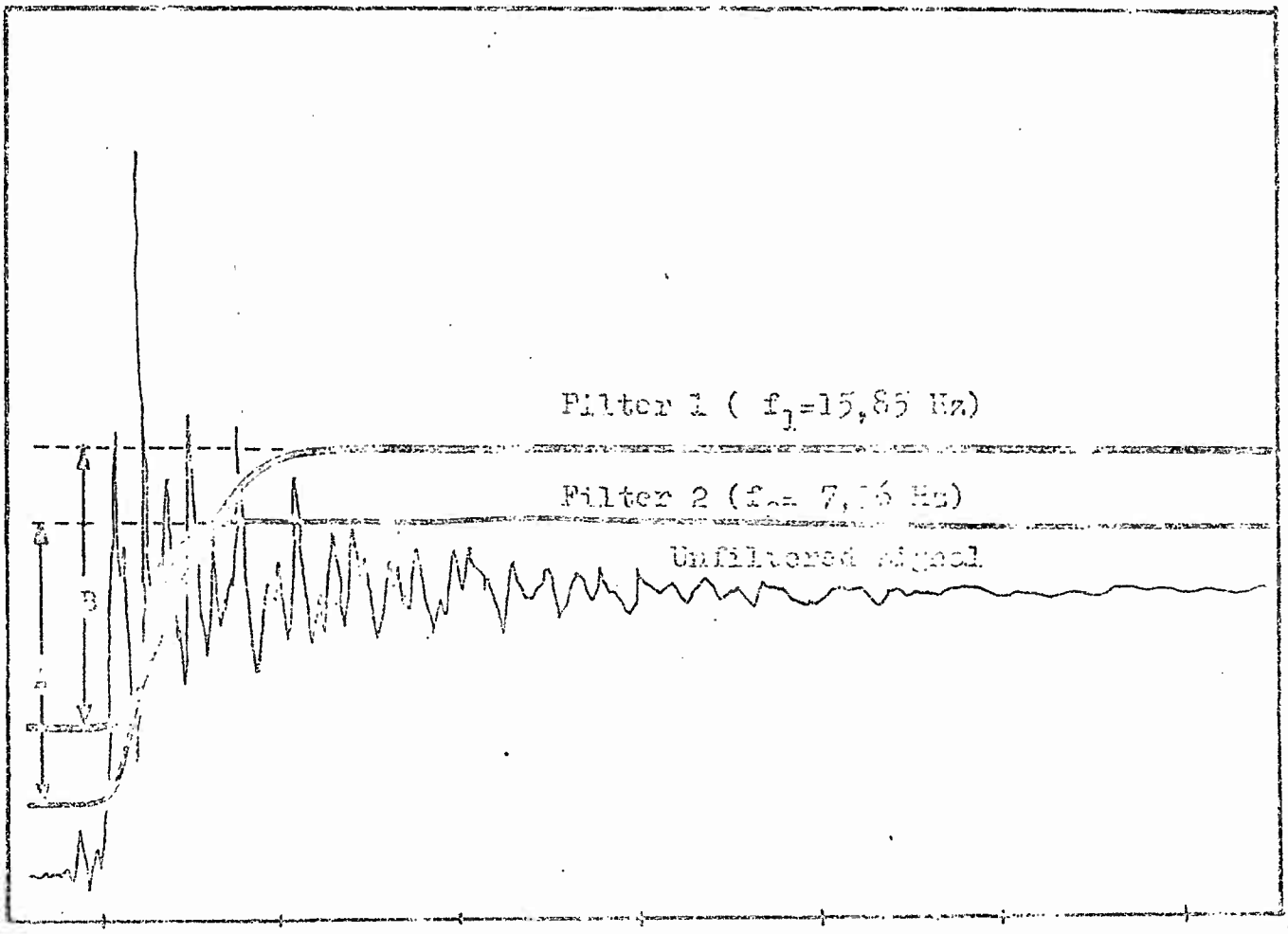

A=80 bar
B=78 bar
} A/B = 1,02

FIG. E.4. Unfiltered and filtered signals due to direct hammer blow.

Table 4.2. System specifications

Transducer	Range (bar)	Linearity
Kistler 6201	0-5000	± 0,4%
Kistler 601 H	0-1000	± 0,4%
Kistler 603 B	0- 200	± 0,5%

Charge amplifiers

Kistler 504 A, 565 and 568 Linearity ± 0,1%

Kistler 5001 Linearity ± 0,05%

Tape recorder Ampex FR 1300 A

Voltage linearity	± 0,75%
Harmonic distortion	± 1,8%
Tape speed distortion	± 0,25%

Galvanometer amplifier

Kistler 5211 Linearity ± 0,4%

U-V writer

CEC type 124-5 Linearity ± 1%

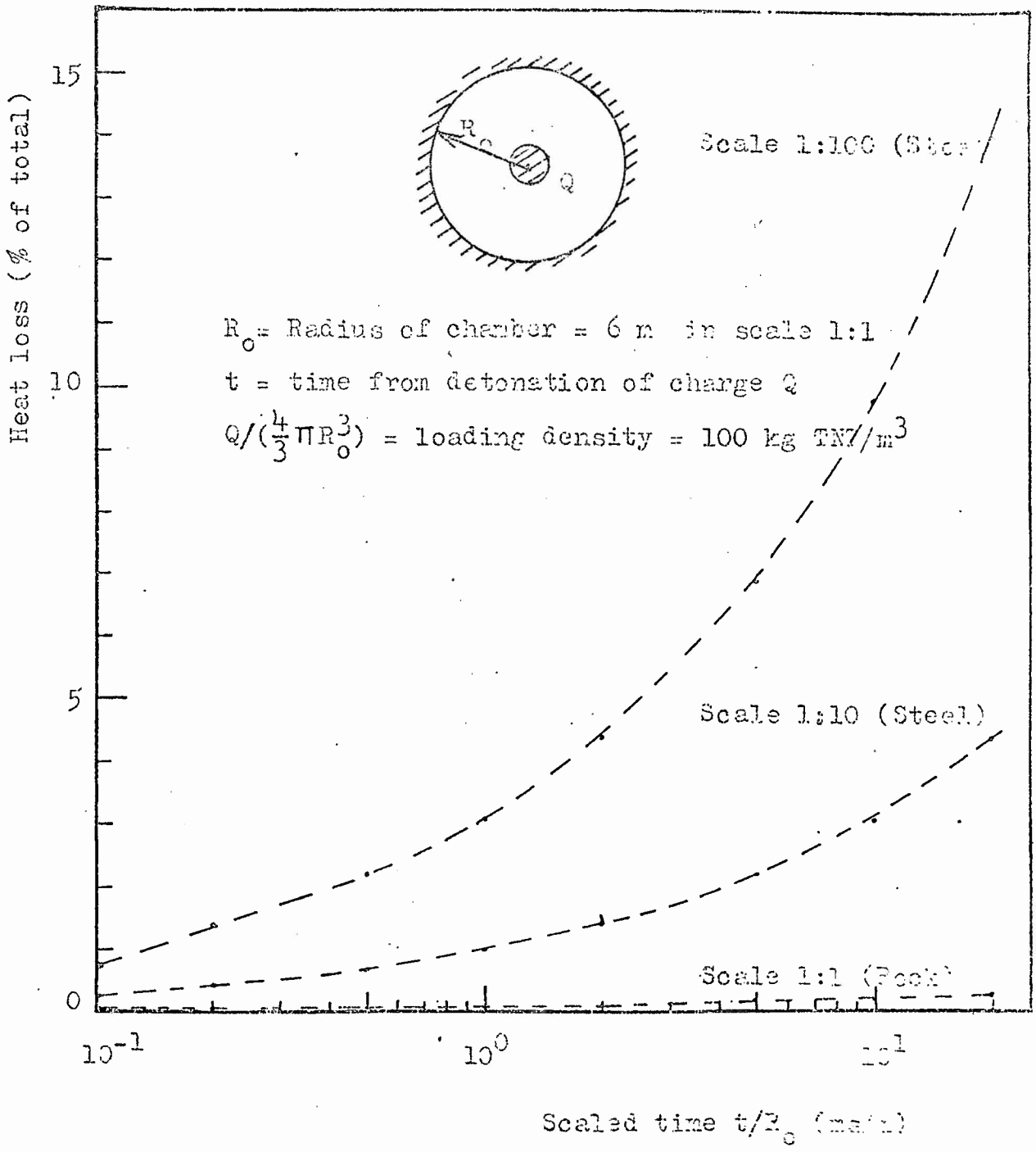

Fig.2.2: Conduction heat loss versus scaled time for a full scale chamber in rock and steel tested in linear scales 1:10 and 1:100, /16/.

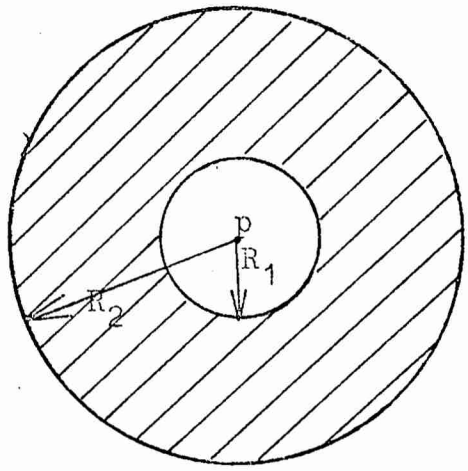

R_1 = internal chamber radius

R_2 = external chamber radius

p = chamber pressure (step load)

	Lamé's constant		Elastic modulus	
	μ_L [a] (N/m^2)	λ_L [b] (N/m^2)	E (N/m^2)	ν
Steel	$8,1 \times 10^{10}$	$12,1 \times 10^{10}$	$2,1 \times 10^{11}$	0,3
Granite	$0,87 \times 10^{10}$	$0,37 \times 10^{10}$	$0,2 \times 10^{11}$	0,15

[a] $\mu = \frac{E/2}{1 + \nu}$, where ν = Poissons ratio

[b] $\lambda = \frac{E \cdot \nu}{(1 + \nu)(1 - 2\nu)}$

Fig. 2.3 Definition of symbols and numerical values used in the calculation elastic deformation energy for a spherical chamber.

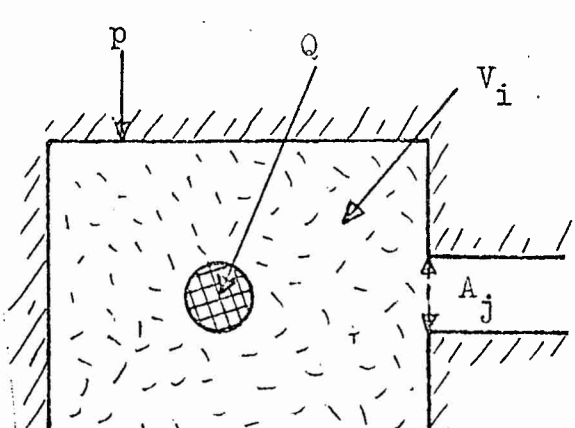

V_i (cm^3)	A_j (cm^2)	Q
4300	≤ 0.1	TNT
7250	35.0	PETN
10900	70.0	AN/FO
15200	81.0	RDX
17300	140.0	ALUMIT
		DYNAMITE
		COMP.B

Fig.3.1: Model configuration used in the closed bomb tests (Report II), with different chamber volumes V_i, vent areas A_j and type of explosive Q.

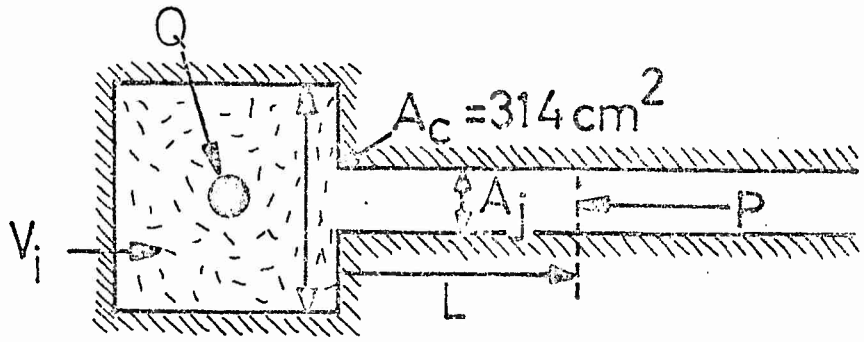

i	V_i (cm^3)	V_i^F (m^3)	j	A_j (cm^2)	A_j^F (m^2)	n
1	7250	380-3100	1	35	20	75
2	10900	580-4700	2	70	20	53
3	15200	800-6500	3	140	20	38

Fig.3.2: Model configurations used in the single chamber storage tests (Report III). The three chamber volumes V_i and the three tunnel cross sections A_j given in the table thus formed nine combinations $V_i A_j$ with i = 1, 2, 3 and j = 1, 2, 3. Choosing A_j^F = 20 m^2 as a typical full scale value for the tunnel cross section, the linear scaling factors n have the values shown in the last column. The corresponding full scale chamber volumes are V_i^F.

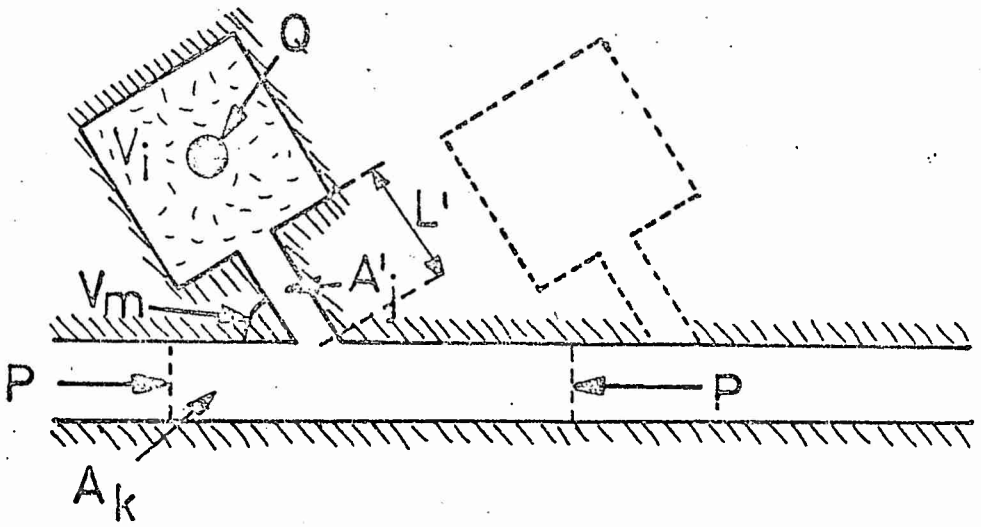

V_i (cm^3)	A_k (cm^2)	A_j' (cm^2)	v_m (deg)
V_1= 300	A_1 = 70	A_1' = 2.5	v_1 = 35
V_2= 800	A_2 = 140	A_2' = 5.0	v_2= 60
V_3= 1760		A_3' = 10.0	v_3= 90
V_4= 7250		A_4' = 70.0	
V_5=10900			
V_6=15200			

Fig.3.3: Model configurations used in the multiple chamber storage tests (Report IV). A total of 18 different combinations were tested varying the chamber volume V_i, the angle v_m between the branch and main passage-way and the ratio between the cross sections of the branch and main passage-way, A_j/A_k. These configurations were:

V_i A_1 A_j' V_3 with i = 1, 2, 3. j = 1, 2, 3.

V_i A_2 A_4' v_m with i = 1, 2, 3. m = 1, 2, 3.

p denotes pressure measurements in the tube.

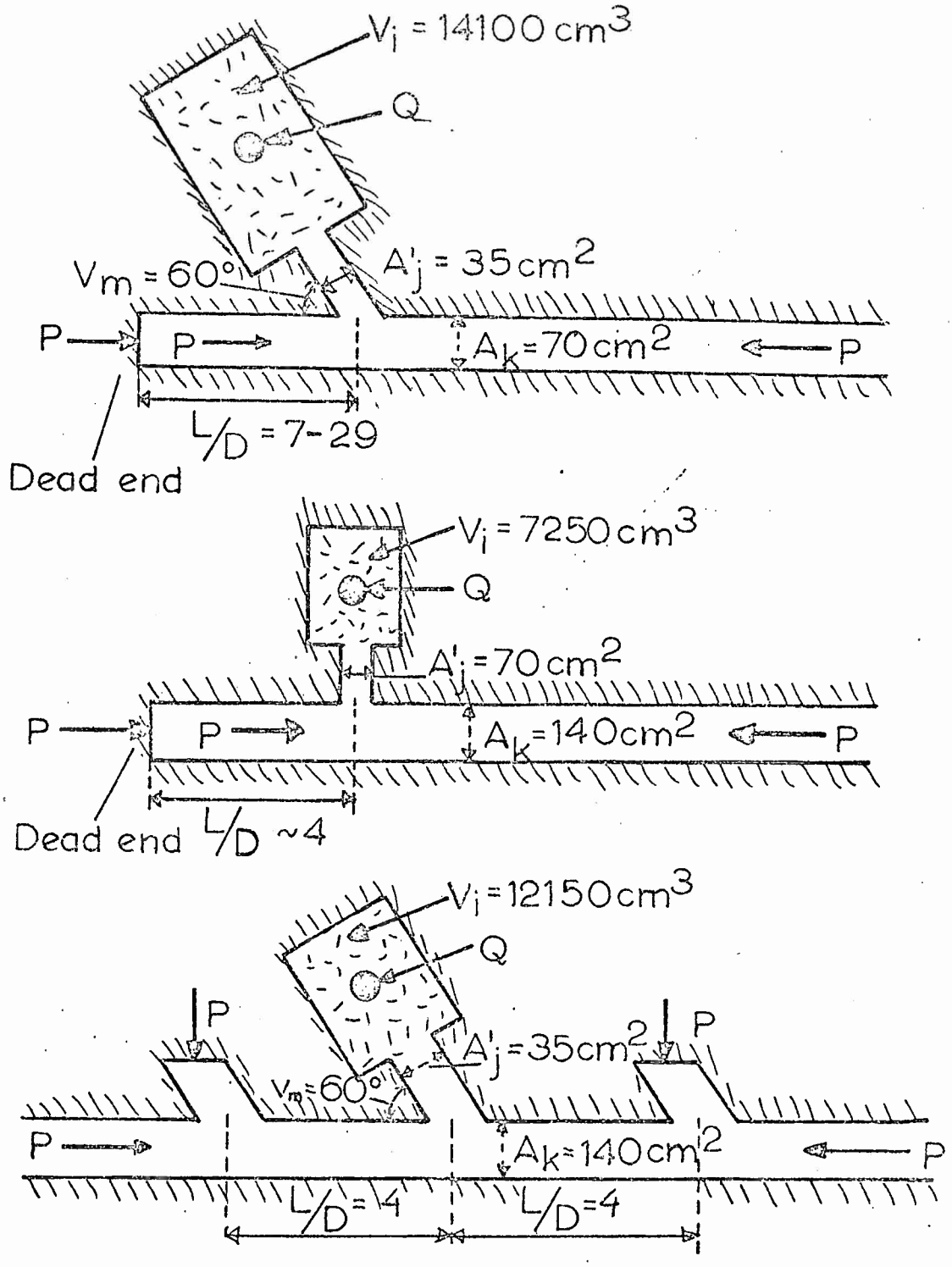

Fig.3.4: Model configuration of the three sites discussed in Report V .
p denotes pressure measurements.

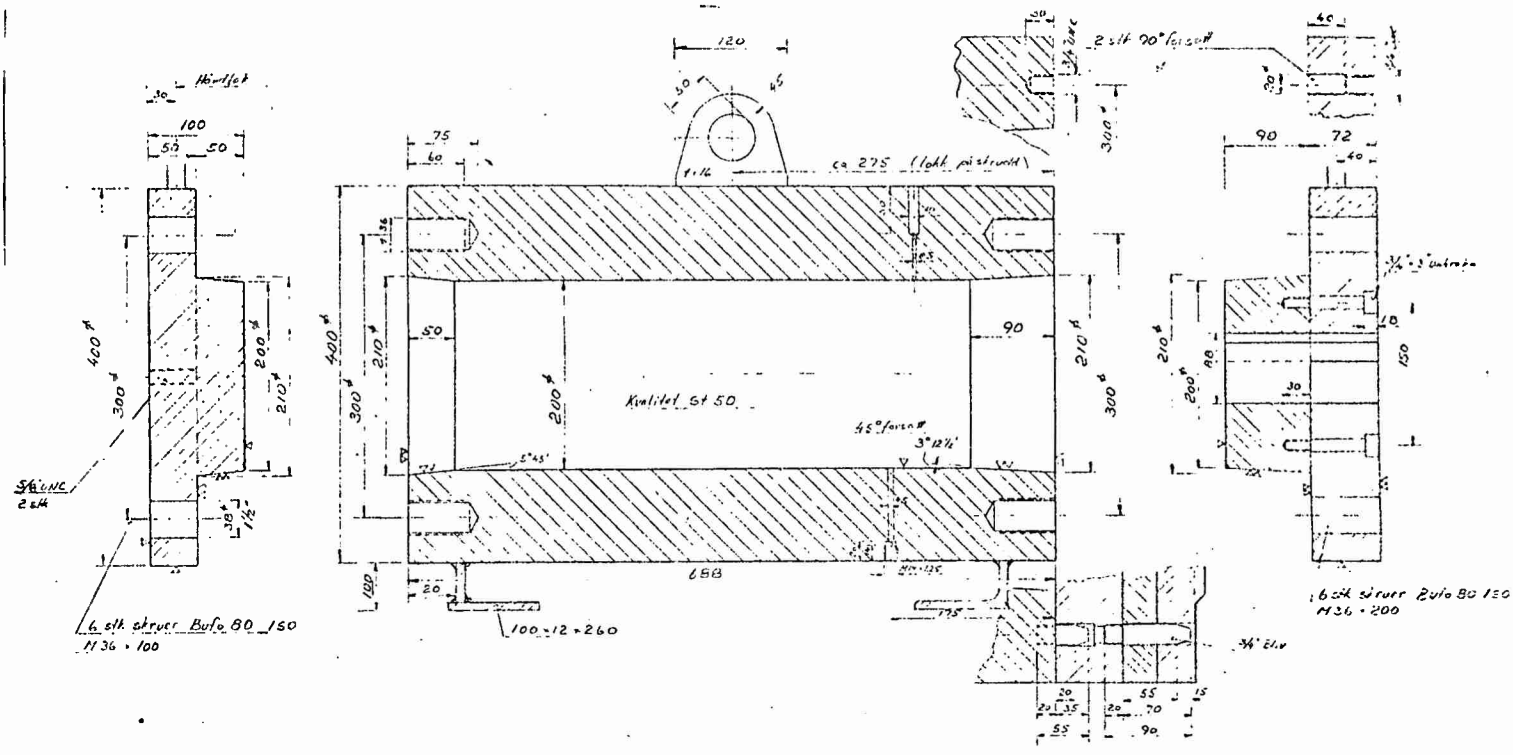

Fig. 3.5 a Details of a typical detonation chamber.

Copy available to DDC does not
permit fully legible reproduction

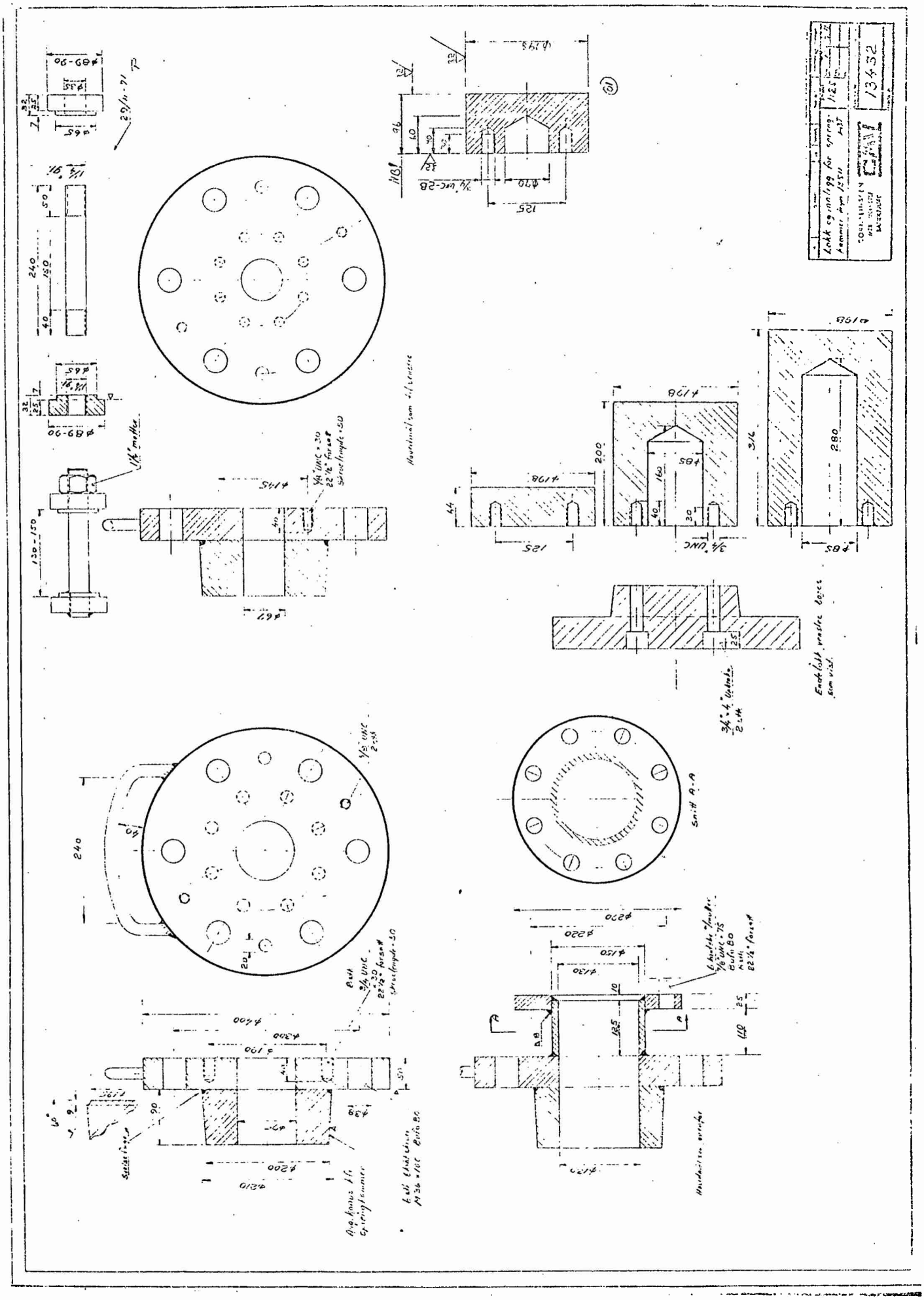

Fig. 3.5 b Details of insertions in detonation chamber.

Copy available to DDC does not
permit fully legible reproduction

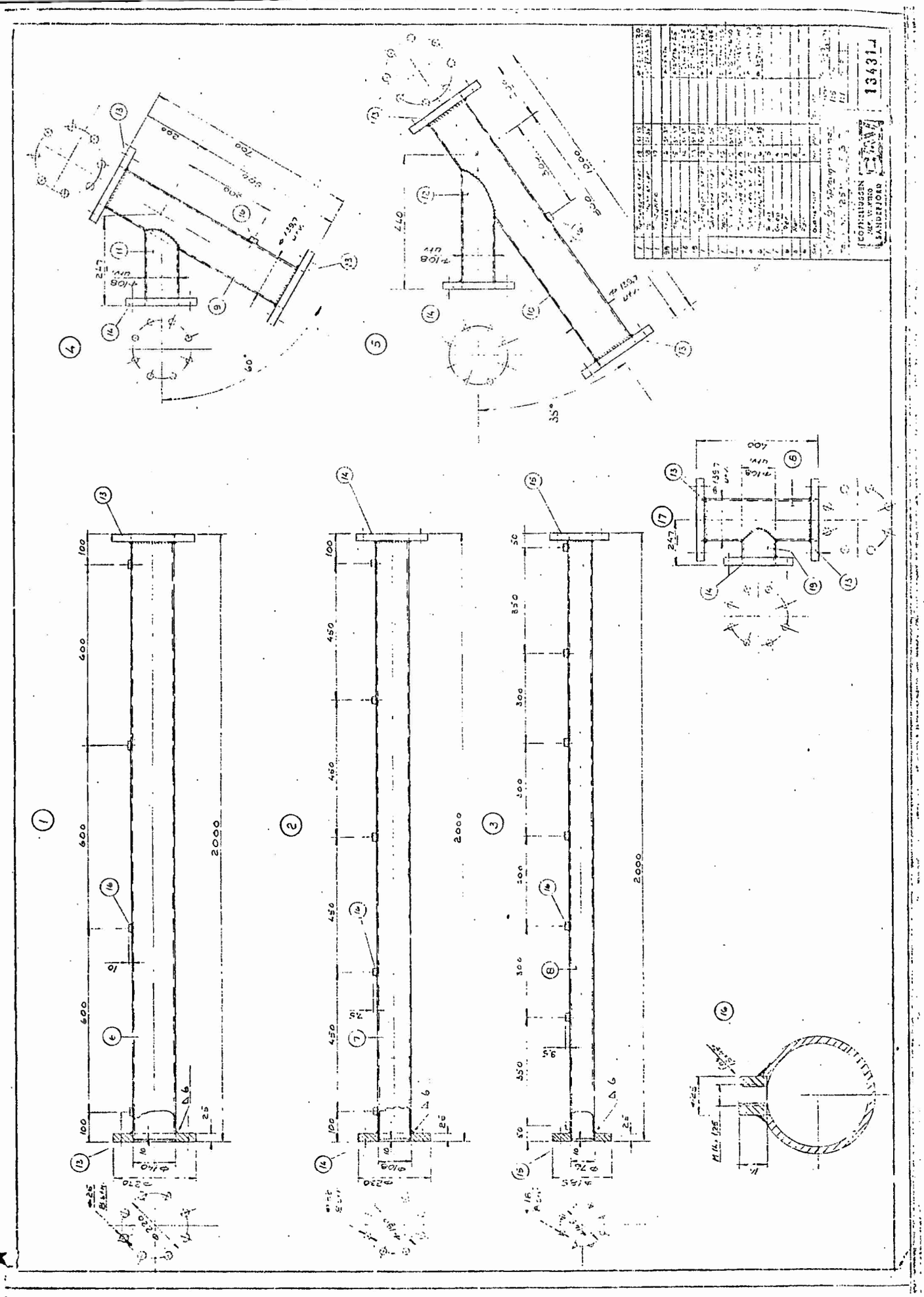

Fig. 3.5 c Details of tube connections.

Copy available to DDC does not
permit fully legible reproduction

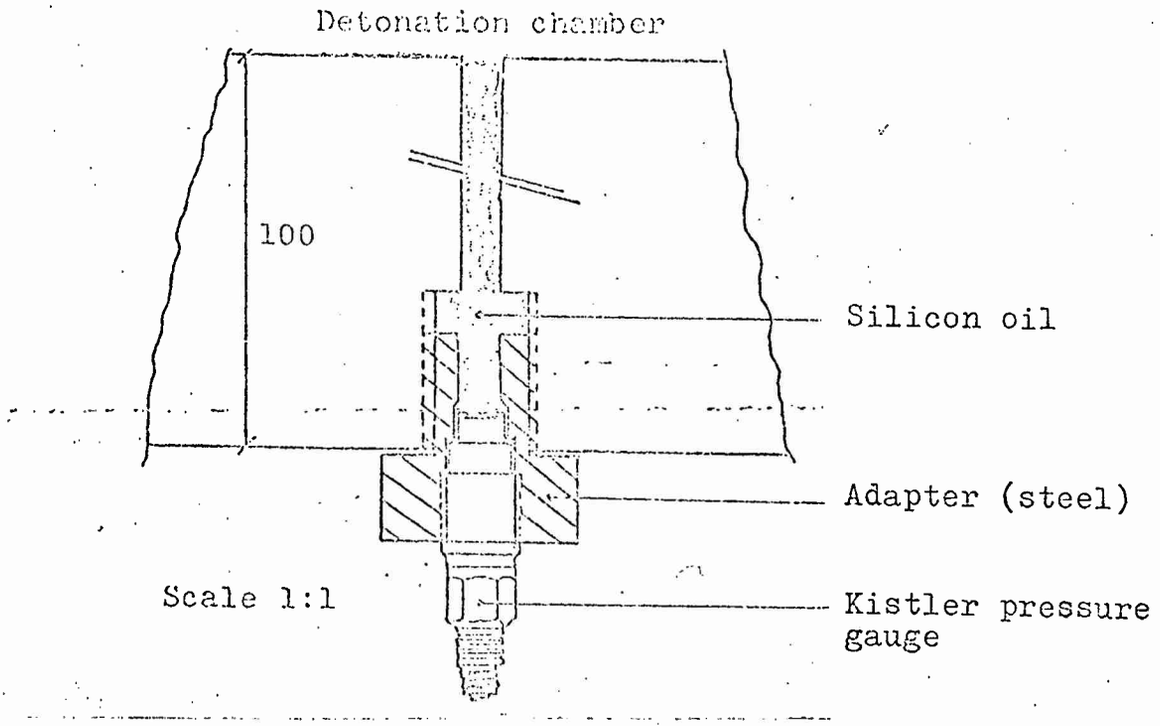

Fig. 4.1 a Heat protection of transducer in detonation chamber.

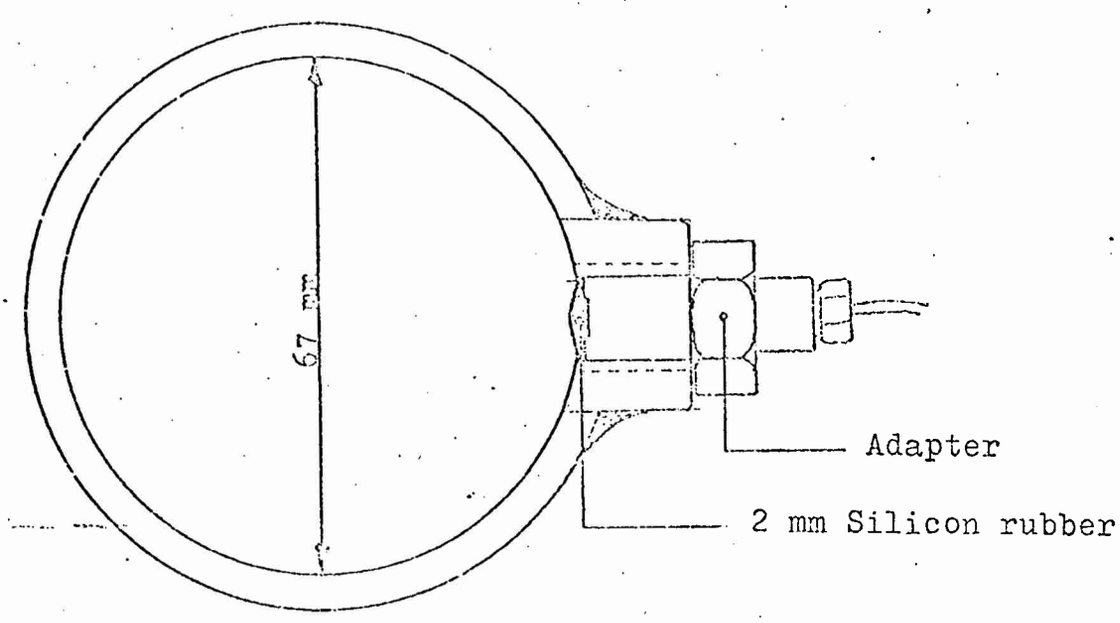

Fig. 4.1 b Section of tunnel with pressure transducer.

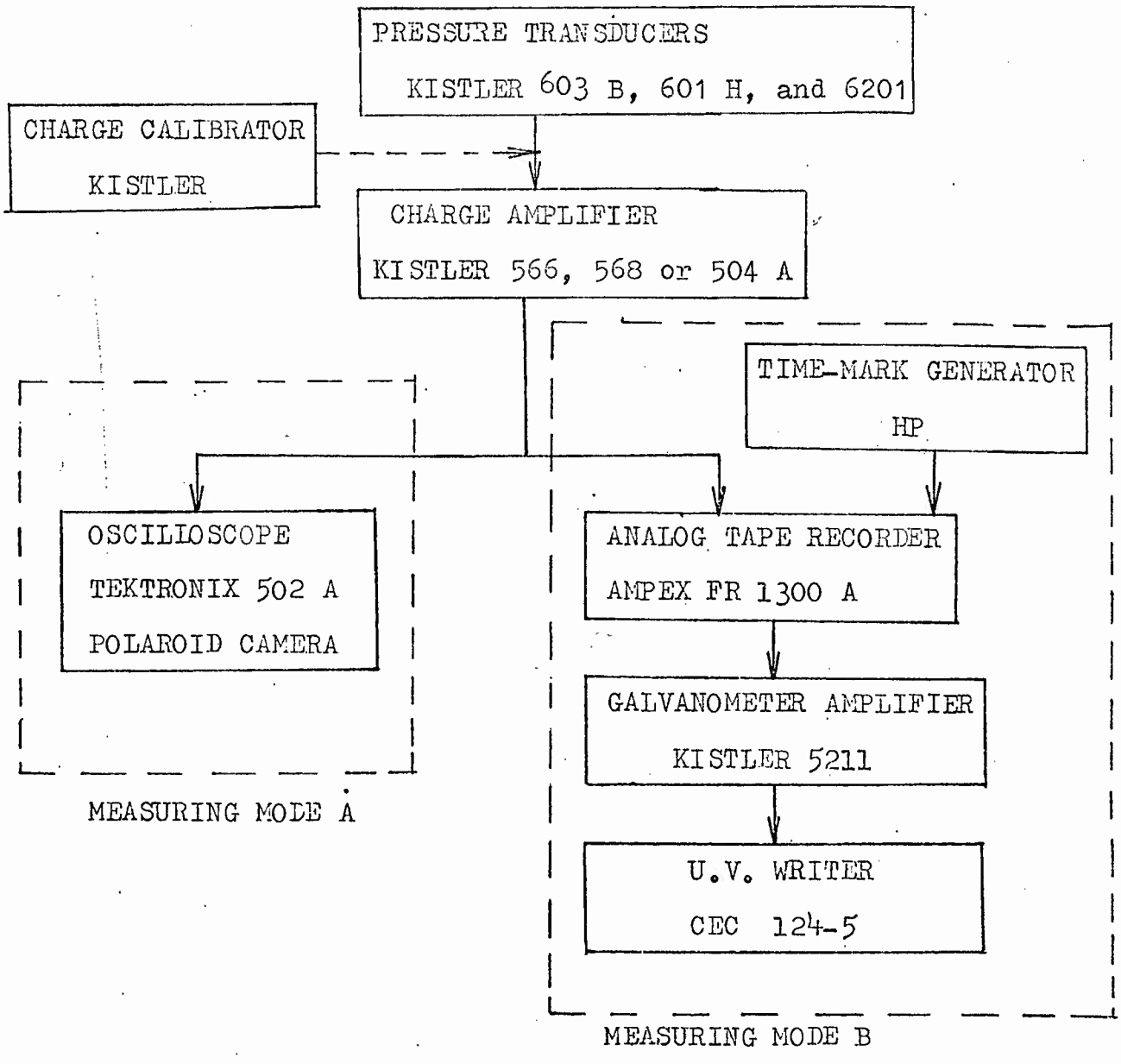

Fig.4.1C: Measuring chain indicating the two different modes used in the tests.